Aquatic Toxicology 205 (2018) 100–113

Contents lists available at ScienceDirect

Aquatic Toxicology

journal homepage: www.elsevier.com/locate/aqtox

Exploring the interactions between polyunsaturated fatty acids and cadmium in rainbow trout liver cells: a genetic and proteomic study

Aline Ferain[a,*], Chloé Bonnineau[b], Ineke Neefs[a], Nancy De Saeyer[c], Benjamin Lemaire[a], Valérie Cornet[d], Yvan Larondelle[a], Karel A.C. De Schamphelaere[c], Cathy Debier[a], Jean-François Rees[a,*]

[a] Louvain Institute of Biomolecular Science and Technology, Université catholique de Louvain, Croix du Sud 2/L7.05.08, B-1348 Louvain-la-Neuve, Belgium
[b] Irstea, UR RiverLy, Centre de Lyon-Villeurbanne, 5, 69625 Villeurbanne, France
[c] Laboratory of Environmental Toxicology and Aquatic Ecology, Environmental Toxicology Unit, Ghent University, Coupure Links 653, B-9000 Ghent, Belgium
[d] Research Unit in Environmental and Evolutionary Biology (URBE), University of Namur, B-5000 Namur, Belgium

ARTICLE INFO

Keywords:
Cadmium
Polyunsaturated fatty acids
RTL-W1 cells
Gene expression
Proteomics

ABSTRACT

Polyunsaturated fatty acids (PUFAs) have key biological roles in fish cells. We recently showed that the phospholipid composition of rainbow trout liver cells (RTL-W1 cell line) modulates their tolerance to an acute cadmium (Cd) challenge. Here, we investigated (i) the extent to which PUFAs and Cd impact fatty acid homeostasis and metabolism in these cells and (ii) possible mechanisms by which specific PUFAs may confer cytoprotection against Cd. First, RTL-W1 cells were cultivated for one week in growth media spiked with 50 µmol L^{-1} of either alpha-linolenic acid (ALA, 18:3n-3), eicosapentaenoic acid (EPA, 20:5n-3), linoleic acid (LA, 18:2n-6) or arachidonic acid (AA, 20:4n-6) in order to modulate their fatty acid profile. Then, the cells were challenged with Cd (0, 50 or 100 µmol L^{-1}) for 24 h prior to assaying viability, fatty acid profile, intracellular Cd content, proteomic landscape and expression levels of genes involved in fatty acid metabolism, synthesis of PUFA-derived signalling molecules and stress response. We observed that the fatty acid supply and, to a lesser extent, the exposure to Cd influenced cellular fatty acid homeostasis and metabolism. The cellular fatty acid composition of fish liver cells modulated their tolerance to an acute Cd challenge. Enrichments in ALA, EPA, and, to a lesser extent, AA conferred cytoprotection while enrichment in LA had no impact on cell viability. The present study ruled out the possibility that cytoprotection reflects a decreased Cd burden. Our results rather suggest that the PUFA-derived cytoprotection against Cd occurs through a reduction of the oxidative stress induced by Cd and a differential induction of the eicosanoid cascade, with a possible role of peroxiredoxin and glutaredoxin (antioxidant enzymes) as well as cytosolic phospholipase A2 (enzyme initiating the eicosanoid cascade).

1. Introduction

Cadmium (Cd) is an ubiquitous heavy metal that is toxic to human and wildlife. In fish, liver and kidney are the primary organs of accumulation under acute and chronic Cd exposure, respectively (Chowdhury et al., 2003). Cytotoxicity of Cd is mainly driven by (i) disruption of ion homeostasis, (ii) modulation of protein structure and properties and (iii) oxidative stress generation. Indeed, Cd binds to sulfhydryl, carboxyl and phosphate groups in proteins and competes with essential metals (e.g. zinc, calcium, manganese and selenium), leading to enzyme dysfunction, decreased antioxidant defence, loss of redox balance and ultimately apoptosis (Casalino et al., 2002; Matović et al., 2015; McGeer et al., 2011; Moulis, 2010; Wang et al., 2015). Research indicates that these adverse effects of Cd can be alleviated by nutrition (e.g. supplementation with essential metals, vitamins, phenolic compounds and vegetable oils) (Amamou et al., 2015; Choi et al., 2002; Eriyamremu et al., 2008; Fox, 1979; Jamwal et al., 2016; Linhartova et al., 2016; Linhartova and Sampels, 2015; Peraza et al., 1998).

Lipids, and their constitutive fatty acids, are important components of fish diets, with vital cellular roles. They (i) constitute an important energy source, (ii) directly participate in the maintenance of cell structure and membrane fluidity, (iii) are precursors of signalling molecules and (iv) act as nuclear receptor ligands (Tocher, 2003).

* Corresponding authors.
E-mail addresses: aline.ferain@uclouvain.be (A. Ferain), jf.rees@uclouvain.be (J.-F. Rees).

https://doi.org/10.1016/j.aquatox.2018.09.005
Received 30 July 2018; Received in revised form 7 September 2018; Accepted 10 September 2018
Available online 22 September 2018
0166-445X/

Pollutants, such as Cd, may interfere with these functions. For example, Cd has been reported to modulate cellular fatty acid metabolism, with consequences for tissue and cellular fatty acid composition (Chen et al., 2013; Fadhlaoui and Couture, 2016; Fadhlaoui et al., 2018; Konar et al., 2010; Koskinen et al., 2004; Madejczyk et al., 2015). On the other hand, using an *in vitro* model (rainbow trout liver cell line RTL-W1), we recently showed that cells of which the phospholipids had been enriched in alpha-linolenic acid (ALA, 18:3n-3), eicosapentaenoic acid (EPA, 20:5n-3) or docosahexaenoic acid (DHA, 22:6n-3) were significantly more tolerant to an acute Cd challenge while enrichment in linoleic acid (LA, 18:2n-6) or arachidonic acid (AA, 20:4n-6) had no impact (Ferain et al., 2016). In line with this result, it has been reported that a mixture of EPA and DHA protected human hepatocellular cells (Hep G2 cell line) against acute Cd challenges (24 or 48 h) (Linhartova and Sampels, 2015). Studies with individual polyunsaturated fatty acids (PUFAs) are required to illuminate the mechanisms underlying this protective effect. Actually, numerous sites of interactions between PUFAs and Cd may explain the observed cytoprotection. First, by modifying the physicochemical properties of the plasma membrane (e.g. fluidity, permeability) (Arts and Kohler, 2009; Kremmyda et al., 2011), PUFAs may influence Cd uptake and/or excretion and thereby alter cytotoxicity. Second, PUFAs, as precursors of signalling molecules and ligands of nuclear receptors (Kremmyda et al., 2011; Tocher, 2003), may also promote activation of cellular defences. Importantly though, PUFA-rich biological membranes are prone to oxidative stress (i.e. lipid peroxidation). This could increase risks of cytotoxic effects in fish cells exposed to pro-oxidant metals such as Cd.

The present study therefore aimed at investigating (i) the extent to which PUFAs and Cd impact fatty acid homeostasis and metabolism in fish liiver cells and (ii) possible mechanisms by which specific PUFAs may confer cytoprotection against Cd. To this end, RTL-W1 cells were first differentially enriched in a specific PUFA (ALA, EPA, LA or AA) prior to an acute Cd challenge (24 h). Assays included cellular viability, Cd burden, fatty acid composition, proteome landscape and expression of genes involved in fatty acid metabolism, PUFA-derived signalling and stress response.

2. Material and methods

2.1. Experimental design

The experimental sequence used was the following: (i) fatty acid profile manipulation by incubating RTL-W1 cells for one week in a control or PUFA-enriched (ALA, EPA, LA or AA) medium; (ii) Cd challenge during 24 h and (iii) endpoints assessment: cytotoxicity (n = 6), intracellular cadmium concentration (n = 4), fatty acid profile (n = 3), targeted gene expression (n = 4) and untargeted proteomic analysis (n = 3). The entire sequence (i, ii and iii) was repeated independently up to 6 times (n), depending on the endpoint measured.

2.2. Cell culture and PUFA enrichment

The RTL-W1 cell line was kindly provided by S. Bony (INRA, France). Cells were routinely grown at 19 °C in 175 cm^2 flasks (Cellstar, Greiner Bio-One, Belgium) containing 25 mL of Leibovitz's L15 medium supplemented with 5% foetal bovine serum (FBS; PAA Laboratories, France) and 1% antibiotics (100 IU mL^{-1} penicillin, 100 µg mL^{-1} streptomycin) as detailed earlier (Ferain et al., 2016). Cells from passage 54 to 64 were used in the present study. Cell counts and routine viability measurements were made on disposable hemocytometers (C-chip Neubauer improved, NanoEnTek, USA) using Trypan Blue as exclusion dye.

PUFA enrichment was carried out as previously described (Ferain et al., 2016). Briefly, when 80% confluence was reached, RTL-W1 cells maintained in routine growth conditions were harvested with trypsin 0.0625% in a phosphate buffered solution containing 0.03% ethylenediamine tetraacetic acid (PBS-EDTA) and seeded at a density of 2×10^4 living cells cm^{-2} in 25 mL of growth medium in 175 cm^2 flasks. Growth medium consisted in Leibovitz's L15 medium supplemented with 2% FBS, 1% antibiotics. For the PUFA-enriched conditions, growth medium was spiked with individual PUFAs (either ALA, EPA, LA or AA, 50 µmol L^{-1}). Prior to this, PUFAs (Larodan, Sweden) were complexed with fatty acid free-bovine serum albumin (FAF-BSA) at a molar ratio of 4 to 1 (PUFAs to FAF-BSA), as described by Best et al. (2006). Control cells were supplied with a FAF-BSA level (12.5 µmol L^{-1}) similar to that of PUFA-enriched cells. PUFA enrichment lasted one week during which the growth media were renewed twice.

2.3. Cd challenge

Stock solutions of $CdCl_2$ (0, 5 and 10 mmol L^{-1}, CAS 7790-78-6, Fisher Chemical, UK) were prepared in cell culture grade water and kept at 4 °C in the dark until use. The contaminated media were prepared fresh daily by diluting stock solutions 100 times with L15/ex medium, a restrictive medium containing salts, galactose and pyruvate at the same concentration as the Leibovitz's L15 medium (Dayeh et al., 2002). After one week of PUFA enrichment (see Section 2.2), the growth media were replaced by 25 mL of contaminated media (0, 50 or 100 µmol L^{-1} Cd). These contamination levels were chosen within the range in which ALA and EPA enrichment conferred cytroprotection against Cd (Ferain et al., 2016). Actual contamination levels were measured by inductively coupled plasma atomic emission spectrometry (ICP-AES) (see Section 2.5). After 24 h of Cd exposure, RTL-W1 cells were sampled for downstream analyses. Besides, 24 h cytotoxicity induced by the two doses of Cd tested was assessed using both the Cell-Titer-Blue (CTB) (Promega, The Netherlands) and the 5-carboxy-fluorescein diacetate, acetoxymethyl ester (5-CFDA,AM), (Life Technology, USA) assays, as previously explained (Ferain et al., 2016).

2.4. Cell sampling

After 24 h of Cd exposure, RTL-W1 cells were washed with 10 mL of PBS-EDTA, detached from the flask with trypsin (0.0625% in PBS-EDTA), washed once with ice-cold FAF-BSA (10 g L^{-1} in Leibovitz's L15 medium) and once with L15/ex medium. From each cell suspension, 4×10^6 cells were directly used for fatty acid profile analysis, while the remaining cells were subdivided into aliquots of 1–2 $\times 10^6$ cells each. The aliquots were then centrifuged (400 *g*, 5 min, 19 °C) and cell pellets were flash-frozen in liquid N_2 and kept at -80 °C until downstream analyses (intracellular Cd concentration, gene expression, proteomic analysis).

2.5. Cd quantification

Cd quantification was performed by ICP-AES and, for the non-exposed cells only, by graphite furnace atomic absorption spectrometry (GFAAS). Frozen cell pellets, containing 1×10^6 cells, were re-suspended in Tris Buffer (0.05 mmol L^{-1}, pH 6.8). From this suspension, one aliquot was used for Cd quantification while another one was used for protein quantification (Bradford, 1976). The former was first digested with 100 µL HNO_3 (65%) at 80 °C for 3 h and then diluted to 2.5 mL with deionized water. ICP-AES analyses were run on an iCap 7200 duo spectrophotometer (Thermo Scientific, UK) with argon as plasma gas. Wavelengths for Cd detection were 228.802 nm and 226.502 nm, with the torch in the axial position. GFAAS analyses were run on an ICE3500 spectrophotometer (Thermo Scientific, UK) with argon. A matrix modifier ($MgNO_3$, 5 µL, 4 g L^{-1}) was added to the samples (15 µL). The temperature program was as follows: (i) drying at 110 °C for 35 s, 130 °C for 10 s, (ii) pyrolysis at 450 °C for 20 s, (iii) atomisation at 1500 °C for 3 s and (iv) cleaning at 2500 °C for 3 s. During the atomisation step, Cd atomic absorption was measured at 228.802 nm, with a Zeeman background correction. For both ICP-AES

and GFAAS analyses, Cd concentration was calculated thanks to a calibration curve made from certified standards (Fluka, Germany). Besides, the accuracy of the whole process was controlled both by the standard addition method (recovery 93 ± 2%) and by the analysis of reference materials (TM-28.4 and TMDA-70.2, Environment Canada, Canada) every 25 samples (recovery 99 ± 1% in ICP-AES and 96 ± 3% in GFAAS). For each experimental condition from each biological replicate, quantification was performed on two independent frozen cell pellets. Data from these technical duplicates were averaged. The Cd concentration in contaminated media was also determined by ICP-AES. Exact contamination levels were 48.7 ± 1.0 and 98.0 ± 2.1 µmol L^{-1}.

2.6. Cellular fatty acid profile determination

After centrifugation (800 *g*, 6 min, 19 °C), the freshly sampled 4×10^6 cells were resuspended in 2 mL of L15/ex medium from which 0.1 mL was used for protein quantification and 2 x 0.8 mL was used for lipid extraction (analyses were performed in duplicate). The 0.1 mL aliquots were centrifuged (550 *g*, 5 min, 4 °C). The isolated cell pellet was lysed (ice-cold lysis buffer: 60 mmol L^{-1} Tris, 10 mmol L^{-1} EDTA, 1% sodium dodecyl sulphate (w/w) in water) and stored at -20 °C until protein quantification using the Bicinchoninic acid (BCA) Protein Assay (Thermo Scientific Pierce, USA), with BSA as standard.

Cellular total lipids were first extracted with methanol:-chloroform:water (2:2:1.8, v:v:v) (Bligh and Dyer, 1959), then separated into neutral lipids, free fatty acids and phospholipids (Schneider et al., 2012) and finally methylated (Ferain et al., 2016). The resulting fatty acid methyl ester (FAMEs) from the neutral lipids and phospholipid fractions were extracted (Ferain et al., 2016) and separated by gas chromatography (Ferain et al., 2018) The chromatograph (GC Trace-1310, Thermo Fisher Scientific, Italy) was equipped with a RT2560 capillary column (100 m x 0.25 mm internal diameter, 0.2 µm film thickness: Restek, USA), a TriPlus TP100 autosampler (Thermo Fisher Scientific, Italy) and a flame ionisation detector (FID: Thermo Quest, Italy). The carrier gas used was H_2 at constant pressure (200 kPa) and flow rate (2 mL min^{-1}). The FID was continuously flowed by H_2 (35 mL min^{-1}), air (350 mL/min) and N_2 (40 mL min^{-1}) and kept at a constant temperature of 255 °C. The temperature program was as follows: an initial temperature of 80 °C, which increased at 25 °C min^{-1} up to 175 °C, a holding temperature of 175 °C during 25 min, a new increase at 10 °C min^{-1} up to 200 °C, a holding temperature of 200 °C during 20 min, a new increase at 10 °C min^{-1} up to 220 °C, a holding temperature of 220 °C during 5 min, a last increase at 10 °C min^{-1} up to 235 °C and a final holding temperature of 235 °C during 15 min. FAMEs were finally identified and quantified by comparing the obtained chromatograms (retention times and peak areas) with that of a standard containing 44 FAMEs (Larodan, Sweden) at known concentrations. The chromatogram management software used was ChromQuest (version 5.0, ThermoFinnigan, Italy). Data from the technical duplicates were averaged.

2.7. Gene expression

Total RNA was extracted from 1×10^6 frozen cells using the Aurum Total RNA Mini Kit (Bio-Rad Laboratories, USA) following manufacturer's Spin Protocol. The DNAse I treatment was always included. RNA quality and quantity was assessed spectrophotometrically on a Nanodrop ND-1000 (Isogen, Life Sciences, The Netherlands) using the optical densities (OD) measured at 260, 280 and 230 nm (OD_{260}, $OD_{260/280}$ and $OD_{260/230}$). Total RNA (1 µg) was then reverse transcribed with the Iscript cDNA Synthesis Kit (Bio-Rad Laboratories, USA) according to manufacturer's instructions. cDNA was diluted 3 times in nuclease free water and kept at -20 °C until quantification of the expression level of targeted genes (Table 1). Quantitative polymerase chain reactions (qPCR) were run on a Step One Plus thermocycler (Applied Biosystems, Life Technologies, USA). Samples were run in technical duplicates. Each reaction contained cDNA (1 µL), primers and SYBR Select Master Mix I (Applied Biosystems, Life Technologies, USA) in a final volume of 20 µL. The temperature programme was: (i) 95 °C for 2 min, (ii) 95 °C for 15 s, (iii) gene-specific annealing-extension temperature (see Table 1) for 1 min. Steps (ii, iii) were repeated 40 times. The programme ended with a melt curve analysis. Primer pairs for 16 target genes and 2 housekeeping genes (Table 1) were either obtained from literature or designed using transcript sequence information available at the European Nucleotide Archive (for identifiers, see Marancik et al. (2014)). The targeted genes are involved in fatty acid uptake (fatty acid transport protein 1 (*FATP1*)), fatty acid *de novo* synthesis (fatty acid synthase (*FASN*)), fatty acid bioconversion (fatty acid desaturase 2 (*FADS2*), fatty acid elongases 2 and 5 (*ELOVL2* and *ELOVL5*)), β-oxidation (carnitine palmitoyl transferase 1 (*CPT1*)), synthesis of PUFA-derived signalling molecules (cytosolic phospholipase A2 (*cPLA2*), cyclooxygenase 2 (*COX2*), arachidonate 5-lipoxygenase (*ALOX5*)) and stress response (metallothioneins a and b (*MTa* and *MTb*), heat shock proteins 70a and 70b (*HSP70a* and *HSP70b*), apoptosis regulator BCL2-Like1 (*BCLx*), tumor protein 53 (*p53*), calreticulin (*CALR*)) (Fig. 1). The orphan cytochrome P450 20A1 gene (*CYP20A1*) was also studied. Each primer pair used was experimentally validated: (i) the linearity of the amplification was assessed, (ii) optimum primer concentrations were determined and (iii) the identity of the amplified sequence was confirmed by sequencing (Beckman Coulter Genomics, UK). Relative expression analysis was performed with the $E^{-\Delta\Delta Ct}$ method (Livak and Schmittgen, 2001). For each biological replicate, Ct values of technical duplicates were averaged prior to relative expression calculation. The geometric mean of *tubulin* and *18S* Ct values was used as housekeeping value (Vandesompele et al., 2002). Other genes and gene combinations tested as housekeepers were proved unreliable (i.e. lower stability of Ct values across treatments; data not shown). Control cells that were not exposed to Cd were used as reference condition, for relative expression of data. An arbitrary expression value of 1 was given to each biological replicate of this condition. Note that for *MTa*, the reference condition for relative expression of data was control cells exposed to 50 µmol L^{-1} Cd as no detectable signal of amplification could be obtained for in the absence of Cd challenge. The *MTa* expression level of the latter experimental condition was set at 1 for each biological replicate.

2.8. Proteomic analysis

A subset of 8 experimental conditions was selected for proteomic analysis (CT, ALA-, EPA- and AA-enriched cells, exposed to either 0 or 50 µmol L^{-1} Cd). Sample analysis was carried out as described by Villers et al. (2017), with minor adaptations. Briefly, frozen cell pellets (1×10^6 cells) were resuspended in tetraethylammonium bromide buffer (TEAB, 0.5 mol L^{-1}, pH 8.0, Thermo Scientific, USA) containing a protease inhibitor (Halt Protease and Phosphatase Inhibitor Cocktail, Thermo Scientific, USA), homogenized (15 s, Vortex), sonicated (30 s) and centrifuged (90,720 *g*, 30 min, 4 °C, Optima ultra-speed centrifuge equipped with a TLA-55 rotor, Beckman Coulter, USA). Supernatants containing soluble proteins were isolated. Proteins were quantified with the BCA Protein Assay, using BSA as standard. Soluble proteins (20 µg) were digested and labelled for iTRAQ (8-plex) as described by Villers et al. (2017). Samples (8) from the same biological replicate were then pooled and labelled peptides were separated by reversed phase chromatography on a C18 PepMap100 pre-column and analytical column (LC Packings, The Netherlands) for 180 min at a flow rate of 300 nL min^{-1} using a linear gradient from 8% acetonitrile in water/0.1% trifluoroacetic acid to 76% acetonitrile in water/0.085% trifluoroacetic acid. The eluted peptides were mixed with α-cyano-4-hydroxycinnamic acid matrix (2 mg mL^{-1} in 70% acetonitrile, 0.1% trifluoroacetic acid) and spotted directly onto a MALDI target using a Probot system (LC Packings The Netherlands) (Villers et al., 2017). The spotted plate was

Table 1
Sequence, amplicon size, annealing temperature and optimal concentration in master mix for the primers of the genes investigated.

Gene	Sequence 5'→3'	Size (bp)	Annealing T (°C)	Concentration (nmol L^{-1})	Reference
Tubulin	F: GGTCAATGTGGAAATCAGATCG	111	60	300	*Present study*
housekeeping gene 1	R: TCTCTCAAGCTGCAGATCG				
18S	F: CACGCGAGATGGAGCAATAA	96	60	200	*Gagné et al. (2012)*
housekeeping gene 2	R: CGCAGAGTAGACACACGCTGAT				
FASN	F: TGATCTGAAGGCCCGTGTCA	162	60	200	*Kamalam et al. (2013)*
fatty acid synthase	R: GGGTGACGTTGCCGTGGTAT				
FATP1	F: CGAATGCAACTGTAGCATCG	122	60	300	*Ferain et al. (2018)*
fatty acid transport protein 1	R: CTCYGTGGTCTCCTCATCC				
CPT1	F: CTCCTGGAAGAAGAGGTTCATACG	95	60	100	*Ferain et al. (2018)*
carnitine palmitoyl transferase 1a	R: ACTCACCACCACCACCAAAAAC				
FADS2	F: AGGGTGCCTCTGCTAACTGG	175	60	200	*Kamalam et al. (2013)*
fatty acid desaturase 2	R: TGGTGTTGGTGATGGTAGGG				
ELOVL5	F: CCAAGTACATGAGACACAGAC	115	60	100	*Ferain et al. (2018)*
fatty acid elongase 5	R: CACACAGCAGACACCATCTC				
cPLA2	F: GAGATGTCGTTAGAGGTGTG	94	60	200	*Ferain et al. (2018)*
cytosolic phospholipase A2	R: GTCTCTGCGTGTCTGTCTGA				
COX2	F: CATCGGACAAGAACCCTTGA	73	60	100	*Chettri et al. (2011)*
cyclooxygenase 2	R: CTTCATTGGAGAGGCTGGTGTGC				
ALOX5	F: CGGCAGAGCACGGTTGCCAAAG	104	58	200	*Baron et al. (2005)*
arachidonate 5-lipoxygenase	R: CCACTCACTCCATCTGTAGGTT				
HSP70a	F: CAGCATTGAGATTGACTCC	86	60	300	*Ferain et al. (2018)*
heat shock protein 70a	R: GTCAGAACACATCTCCTC				
HSP70b	F: CAGCATTGAGATTGACTCT	71	60	200	*Ferain et al. (2018)*
heat shock protein 70b	R: GTCGGAACACATTTCCTC				
MTa	F: CATGCACCAGTTGTAAGAAAGCA	75	60	300	*Ceyhun et al. (2011)*
metallothionein a	R: GCAGCCTGAGGCACACTTG				
MTb	F: ATCCTGCAAGTGCTCAAACT	139	60	300	*Ceyhun et al. (2011)*
metallothionein b	R: ATGACTGCATTGTCACGGTA				
p53	F: GACAACCCTGGAGACCAAGA	132	60	100	*Hecht et al. (2014)*
tumor protein 53	R: TCTCATCGTCACTCACAGCA				
BCLx	F: GGACTCAGTGGATGAGTTTGAGC	122	60	200	*Ferain et al. (2018)*
apoptosis regulator BCL2-Like1	R: GAACACTTCGTCCATCACACTCTC				
CALR	F: GTTCGGTCCAGACATCTGTG	115	60	300	*Present study*
calreticulin	R: GTGTACTCATCATCCTTGC				
CYP20A1	F: GCTGTCACTCAACTCGCTCTG	137	60	300	*Ferain et al. (2018)*
cytochrome P450 20A1	R: CTGATGGAGCTCTTCTCCATG				

Transcript sequences used for primer design were gleaned from the literature or designed (*"Present study"*) based on transcript sequences annotated by Marancik et al. (2014). (see *"Reference"* column). Abbreviations used: bp, base pairs ; F, forward; R, reverse; T, temperature.

analysed on an 4800 MALDI TOF/TOF Analyzer (Applied Biosystems, Life Technologies, USA) and MS, MS/MS spectra were obtained and processed as described by Villers et al. (2017). LC/MSMS data were confronted to the trout peptide database (http://www.genoscope.cns.fr/trout/data/). The same search options as in Villers et al. (2017) were applied in the analysis method. Results were further processed by the Pro Group™ Algorithm to determine the minimal set of justifiable identified proteins (Villers et al., 2017). Protein identification was confirmed using the Mascot 2.2.04 program (Matrix Science, USA) using the same database as for ProteinPilot (SCIEX, USA). The following variable modifications were allowed: C-carbamidomethyl, K-acetylation, methionine oxidation, dioxidation and trypsin. Proteins were finally annotated based on *Oncrorhynchus_genome* database, and *Oncorhynchus_peptide* database (both available at the genoscope trout genome resources - URL cited above).

2.9. Statistical analyses

Graphs and statistical analyses were performed with the JMP PRO 12.0 software. Variance homoscedasticity and normality of residuals were checked with appropriate tests (Bartlett test, Levene test, Shapiro-Wilk test, skewness and kurtosis calculations) prior to performing parametric tests. Type I error (α) was set at 0.05. A Bonferroni-Sidak correction was applied to correct the p-values in any case of multiple testing (Sidak, 1967).

The fact that metabolic activity, membrane integrity and intracellular Cd concentration of the non-exposed cells as well as gene expression levels of the reference condition had no variance restricted the use of classical statistical tests. This limitation was overcome by performing Student's t-tests (Dagnelie, 2006) to determine (i) whether metabolic activity and membrane integrity were significantly different from 100%, (ii) whether intracellular Cd concentrations were different from 0 and (iii) whether relative gene expression levels were different from 1. In any other case, two one-way ANOVAs were performed to assess impacts of the PUFA enrichment strategy and the Cd exposure level. For each PUFA enrichment strategy separately, a first one-way ANOVA followed by a post-hoc Tukey test was performed to assess impact of the Cd exposure level on membrane integrity, metabolic activity (both arsin-rootsquare transformed), Cd intracellular concentrations (no data transformation required) and gene expressions (Log transformed). For each Cd exposure level separately, the impact of the PUFA enrichment strategy was assessed by a second 1-way ANOVA followed by a post-hoc Dunnett's test, with control cells as reference condition.

Statistical analyses of the proteomic data were performed by combining the p-values computed by ProteinPilot, using weighed z-scores (Zaykin, 2011), as described by Villers et al. (2017).

3. Results

3.1. PUFA enrichment modulates the phospholipid composition of the RTL-W1 cells

The fatty acid profile of RTL-W1 cell phospholipids was modified by changing the PUFA composition of the culture medium (Table 2).

Phospholipids of cells cultivated for one week in a medium enriched

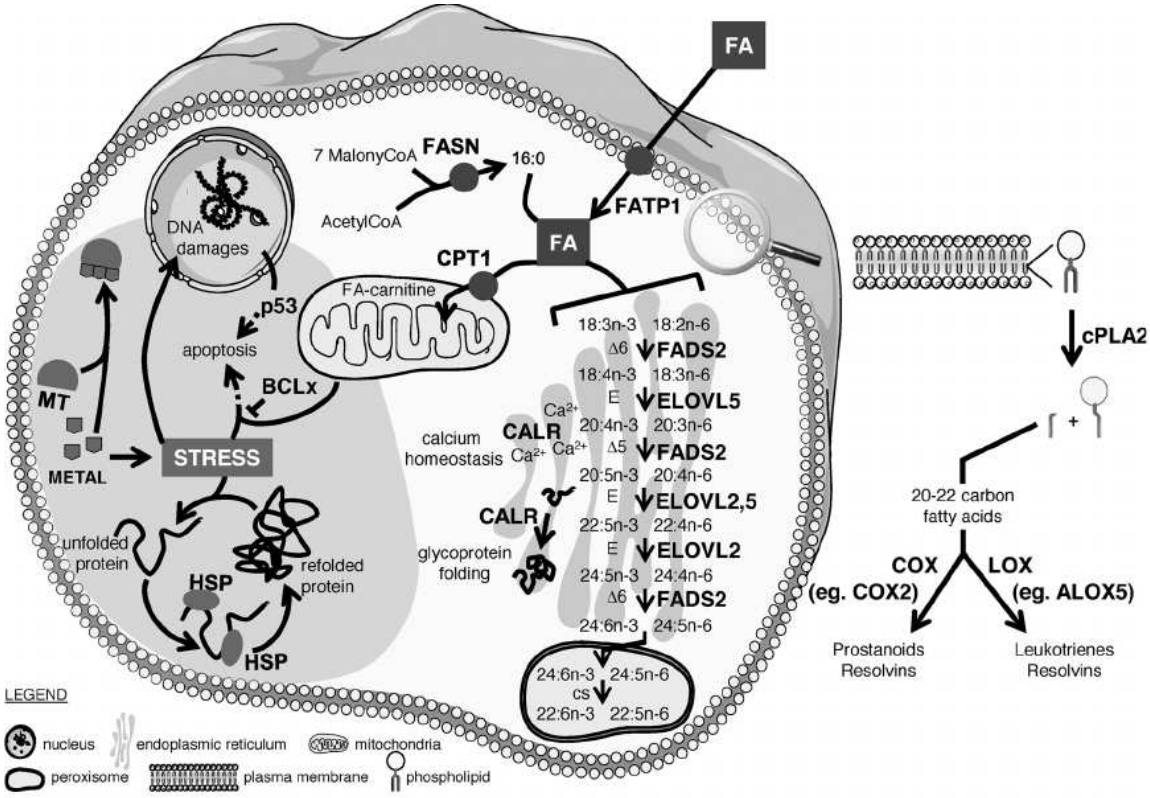

Fig. 1. Roles of the proteins encoded by the genes investigated. The illustration (adapted from Ferain et al. (2018)) has been done using the "cell biology" package from Servier Medical Art. Abbreviations used: Δ5, Δ5 desaturation; Δ6, Δ6 desaturation; ALOX5, arachidonate 5-lipoxygenase; BCLx, apoptosis regulator BCL2-Like1; CALR, calreticulin; COX2, cyclooxygenase 2, cPLA2, cytosolic phospholipase A2; CPT1, carnitine palmitoyl transferase 1; cs, peroxisomal chain shortening; E, elongation; ELOVL2, fatty acid elongase 2; ELOVL5, fatty acid elongase 5; FA, fatty acid; FADS2, fatty acid desaturase 2; FASN, fatty acid synthase; FATP1, fatty acid transport protein 1; HSP, heat shock protein; MT, metallothionein; p53, tumor protein 53.

Table 2
Fatty acid composition of RTL-W1 cell phospholipids after one week culture in a growth medium supplemented or not (control) in a specific PUFA (50 µmol L^{-1} ALA, EPA, LA or AA) followed by 24 h in a medium deprived of fatty acid (µmol g^{-1} protein).

Fatty acids	Control	ALA	EPA	LA	AA
14:0	12.7 ± 3.3	6.0 ± 1.4	10.1 ± 0.9	7.1 ± 0.8	9.2 ± 0.9
16:0	206.6 ± 72.6	154.6 ± 13.9	193.2 ± 10.7	180.1 ± 34.0	175.8 ± 21.4
18:0	129.3 ± 39.8	135.4 ± 6.4	121.4 ± 8.4	132.2 ± 20.1	109.7 ± 18.2
Total SFA	**348.5 ± 115.6**	**296.1 ± 18.4**	**324.7 ± 18.5**	**319.4 ± 54.9**	**294.8 ± 40.0**
16:1n-7	11.6 ± 3.5	0.0 ± 0.0 (*)	6.4 ± 0.3	0.0 ± 0.0 *	5.5 ± 0.3
18:1n-7	27.5 ± 6.9	13.2 ± 0.8 *	20.8 ± 1.4	13.2 ± 0.9 (*)	17.0 ± 1.0
18:1n-9	232.4 ± 42.9	87.6 ± 5.2 *	110.5 ± 6.8 *	67.3 ± 6.2 *	91.5 ± 5.4 *
Total MUFA	**271.5 ± 53.0**	**100.8 ± 6.0** *	**137.7 ± 8.4** *	**80.5 ± 7.1** *	**114.1 ± 6.7** *
ALA 18:3n-3	0.0 ± 0.0	**164.2 ± 2.1** *	0.0 ± 0.0	0.0 ± 0.0	0.0 ± 0.0
18:4n-3	0.0 ± 0.0	52.4 ± 6.5 *	0.0 ± 0.0	0.0 ± 0.0	0.0 ± 0.0
20:3n-3	0.0 ± 0.0	12.9 ± 1.0 *	0.0 ± 0.0	0.0 ± 0.0	0.0 ± 0.0
20:4n-3	0.0 ± 0.0	18.4 ± 0.9 *	11.7 ± 2.1 *	0.0 ± 0.0	0.0 ± 0.0
EPA 20:5n-3	8.2 ± 1.1	36.1 ± 4.2 *	**153.5 ± 18.0** *	3.9 ± 0.7 (*)	0.0 ± 0.0 *
22:5n-3	9.4 ± 1.3	8.0 ± 0.6	90.7 ± 10.3 *	7.2 ± 1.2	7.5 ± 0.7
22:6n-3	14.6 ± 2.4	10.4 ± 0.8	13.0 ± 1.3	10.0 ± 2.0	10.6 ± 3.5
Total n-3 PUFA	**32.2 ± 4.2**	**302.3 ± 10.7** *	**268.9 ± 31.0** *	**21.1 ± 2.5**	**18.0 ± 4.0** (*)
LA 18:2n-6	19.3 ± 3.9	11.8 ± 2.8	11.8 ± 0.9	**282.3 ± 45.8** *	9.6 ± 1.0
18:3n-6	4.1 ± 0.8	0.0 ± 0.0 *	0.0 ± 0.0 *	47.6 ± 2.4 *	4.7 ± 0.3
20:2n-6	0.0 ± 0.0	0.0 ± 0.0	0.0 ± 0.0	12.6 ± 2.2 *	0.0 ± 0.0
20:3n-6	12.8 ± 2.0	0.0 ± 0.0 *	6.0 ± 0.7 *	26.4 ± 2.4 *	12.9 ± 0.6
AA 20:4n-6	20.6 ± 3.4	11.0 ± 1.0 *	16.6 ± 1.2	20.5 ± 1.8	**184.9 ± 18.6** *
22:4n-6	0.0 ± 0.0	0.0 ± 0.0	5.3 ± 0.7 *	0.0 ± 0.0	71.7 ± 4.1 *
Total n-6 PUFA	**56.8 ± 10.1**	**22.9 ± 2.7** *	**39.7 ± 3.5**	**389.3 ± 54.6** *	**283.9 ± 23.7** *
Total PUFA	**89.0 ± 14.2**	**325.1 ± 12.9** *	**308.6 ± 34.6** *	**410.4 ± 57.1** *	**301.9 ± 25.5** *
Total	**709.0 ± 179.7**	**722.0 ± 27.4**	**771.1 ± 57.9**	**810.3 ± 119.1**	**710.7 ± 70.7**
n-3/n-6 ratio	**0.58 ± 0.04**	**13.52 ± 1.31** *	**6.74 ± 0.17** *	**0.06 ± 0.01** *	**0.06 ± 0.01** *

Data are expressed as means ± standard error of mean (n = 3). Stars indicate significant differences between control and PUFA-enriched conditions ($p < 0.05$) while stars into brackets indicate similar trends but without significance ($0.05 < p < 0.1$). Abbreviations used: AA, arachidonic acid; ALA, alpha-linolenic acid; EPA, eicosapentaenoic acid; LA, linoleic acid; MUFA, monounsaturated fatty acid; PUFA, polyunsaturated fatty acid; SFA, saturated fatty acid.

in a specific PUFA were significantly richer in the supplemented PUFA and some of its biotransformation products than control cells (see Fig. 1 for the biotransformation pathway). Particularly, ALA, 18:4n-3, 20:3n-3 and 20:4n-3 were found in the phospholipids of cells grown in a medium enriched in ALA but not in those of control cells. ALA-enriched cells contained also about 4-fold more EPA in their phospholipids than control cells. Phospholipids of cells grown in an EPA-rich medium were about 19-fold richer in EPA than those of control cells. Phospholipids of EPA-enriched cells also contained a significantly higher amount of 22:5n-3 than control cells. Adding LA to the culture medium significantly increased the cell phospholipid content in LA (by about 15-fold), 18:3n-6 and 20:3n-6, without affecting AA phospholipid level. The cell phospholipid richness in AA increased by about 9-fold following AA addition to the growth medium. AA-enriched cells also contained 22:4n-6 in their phospholipids while control cells were deprived of it. As a consequence of these individual changes, the phospholipids of RTL-W1 cells grown in a medium enriched in a specific n-3 PUFA (vs a n-6 PUFA) were characterized by a significantly higher (vs a lower) n-3/n-6 ratio than control cells. The PUFA enrichment strategies applied enabled to obtain RTL-W1 cells with n-3/n-6 ratios encompassing a 200-fold range. Finally, phospholipids of cells cultivated in media enriched in a specific PUFA were significantly richer in PUFAs (about 3.5- to 4.5-fold) and poorer in MUFAs (about 2- to 3.5-fold). The decrease of the total MUFA level observed under PUFA enrichment was mainly due to a lower 18:1n-9 level. The SFA content and the total amount of fatty acids identified in cell phospholipids were not changed upon PUFA enrichment.

3.2. PUFA enrichment modulates the neutral lipid composition of the RTL-W1 cells

Cellular neutral lipid levels were about 10 times lower than phospholipid levels irrespective of the PUFA enrichment strategy (Tables 2, 3). Neutral lipids of control cells were composed of SFAs, MUFAs but were deprived of PUFAs (Table 3). Adding a specific PUFA to the growth medium had no impact on SFA level in cellular neutral lipids but significantly decreased MUFA level (by about 3- to 4.5-fold), especially 18:1n-9, as it did in cellular phospholipids. Higher level of the specific PUFA added to the culture medium was recovered in neutral lipids of PUFA-enriched RTL-W1 cells, as well as direct desaturation products for ALA- and LA-enriched cells and elongation products for EPA- and AA-enriched cells (Table 3).

3.3. Cd has limited impact on the phospholipid composition of RTL-W1 cells

A 24-h exposure to Cd (50 or 100 µmol L^{-1}) had no significant impact on the fatty acid profile of RTL-W1 cell phospholipids. A few trends were however noticed in control, LA- and AA-enriched cells (Table 4). The phospholipid level of 22:6n-3 slightly increased under Cd exposure (24 h, 100 µmol L^{-1}) in control cells (+22% as compared to non-exposed control cells) while it decreased (24 h, 100 µmol L^{-1}) in AA-enriched cells (−44% as compared to non-exposed AA-enriched cells). These opposite variations resulted in a significantly lower 22:6n-3 level in phospholipids of AA-enriched cells challenged with the highest Cd dose tested (100 µmol L^{-1}) as compared to control cells challenged with the same Cd level (−67%) (Table 4). Besides, the 20:3n-6 phospholipid level slightly decreased in LA-enriched cells under Cd exposure (−16 to −24%) while it remained stable in control cells. As a result, the significant difference of 20:3n-6 phospholipid level between LA-enriched and control cells disappeared under Cd challenge (Table 4).

3.4. Cd increases the neutral lipid content in n-6 PUFAs of AA-enriched cells

A 24-h exposure to Cd (50 or 100 µmol L^{-1}) had no significant impact on neutral lipid composition in control, ALA-, EPA- and LA-enriched cells (data not shown). The same phenomenon was observed in AA-enriched cells submitted to 50 µmol L^{-1} of Cd. On the other hand, a 2- to 3-fold increase of the absolute levels of AA, 22:4n-6, n-6 PUFAs and PUFAs in the neutral lipids was noticed in AA-enriched cells submitted to 100 µmol L^{-1} of Cd (Table 5).

3.5. PUFA enrichments modulates cell tolerance to Cd

Cd decreased both RTL-W1 cell viability proxies, that are metabolic activity and membrane integrity (Fig. 2). None of the PUFA enrichments modified the apparent drop in membrane integrity caused by Cd. By contrast, ALA, EPA and AA enrichments significantly modulated cell metabolic activity under Cd challenge (Fig. 2). ALA- and EPA-enriched cells challenged with Cd (50 or 100 µmol L^{-1}) were 1.6- to 1.9-fold more metabolically active than control cells exposed to the same Cd dose. A similar significant cytoprotection was induced by AA enrichment at the lowest Cd dose tested (50 µmol L^{-1}) while no impact of AA enrichment on cellular metabolic activity was observed at 100 µmol

Table 3
Fatty acid composition of RTL-W1 cell neutral lipids after one week culture in a growth medium supplemented or not (control) in a specific PUFA (50 µmol L^{-1} ALA, EPA, LA or AA) followed by 24 h in a medium deprived of fatty acid (µmol g^{-1} protein).

Fatty acid	Control	ALA	EPA	LA	AA
16:0	24.7 ± 6.1	24.0 ± 3.5	21.6 ± 4.3	29.9 ± 7.9	21.2 ± 1.6
18:0	33.2 ± 4.1	31.9 ± 7.7	26.4 ± 6.9	34.6 ± 14.3	28.9 ± 5.0
Total SFA	**57.9 ± 10.2**	**55.9 ± 11.2**	**48.0 ± 11.2**	**64.4 ± 22.2**	**50.2 ± 6.4**
18:1n-9	16.8 ± 0.9	4.6 ± 0.4 *	5.3 ± 0.6 *	4.7 ± 1.2 *	3.5 ± 0.5 *
Total MUFA	**16.8 ± 0.9**	**4.6 ± 0.4** *	**5.3 ± 0.6** *	**4.7 ± 1.2** *	**3.5 ± 0.5** *
ALA 18:3n-3	0.0 ± 0.0	**10.7 ± 1.3** *	0.0 ± 0.0	0.0 ± 0.0	0.0 ± 0.0
18:4n-3	0.0 ± 0.0	5.4 ± 0.8 *	0.0 ± 0.0	0.0 ± 0.0	0.0 ± 0.0
EPA 20:5n-3	0.0 ± 0.0	0.0 ± 0.0	**9.2 ± 1.5** *	0.0 ± 0.0	0.0 ± 0.0
22:5n-3	0.0 ± 0.0	0.0 ± 0.0	5.5 ± 0.8 *	0.0 ± 0.0	0.0 ± 0.0
Total PUFA n-3	**0.0 ± 0.0**	**16.2 ± 1.8** *	**14.6 ± 2.2** *	**0.0 ± 0.0**	**0.0 ± 0.0**
LA 18:2n-6	0.0 ± 0.0	0.0 ± 0.0	0.0 ± 0.0	**19.9 ± 7.2** (*)	0.0 ± 0.0
18:3n-6	0.0 ± 0.0	0.0 ± 0.0	0.0 ± 0.0	4.6 ± 0.5 *	0.0 ± 0.0
AA 20:4n-6	0.0 ± 0.0	0.0 ± 0.0	0.0 ± 0.0	0.0 ± 0.0	**6.0 ± 0.5** *
22:4n-6	0.0 ± 0.0	0.0 ± 0.0	0.0 ± 0.0	0.0 ± 0.0	2.6 ± 0.0 *
Total PUFA n-6	**0.0 ± 0.0**	**0.0 ± 0.0**	**0.0 ± 0.0**	**24.5 ± 7.6** (*)	**8.6 ± 0.5** *
Total PUFA	**0.0 ± 0.0**	**16.2 ± 1.8** *	**14.6 ± 2.2** *	**24.5 ± 7.6** (*)	**8.6 ± 0.5** *
Total	**74.7 ± 11.0**	**76.7 ± 10.1**	**67.9 ± 13.5**	**93.6 ± 31.0**	**62.3 ± 7.0**

Data are expressed as means ± standard error of mean (n = 3). Stars indicate significant differences between control and PUFA-enriched conditions ($p < 0.05$) while stars into brackets indicate similar trends but without significance ($0.05 < p < 0.1$). Abbreviations used: AA, arachidonic acid; ALA, alpha-linolenic acid; EPA, eicosapentaenoic acid; LA, linoleic acid; MUFA, monounsaturated fatty acid; PUFA, polyunsaturated fatty acid; SFA, saturated fatty acid.

Table 4
Fatty acid composition of RTL-W1 cell phospholipids after one week culture in a growth medium supplemented or not (control) in a specific PUFA (50 µmol L^{-1} LA or AA) and a subsequent challenge with Cd (0, 50 or 100 µmol L^{-1}) during 24 h in a medium deprived of fatty acid (µmol g^{-1} protein).

Fatty acids	Control			LA			AA		
	0 µmol L^{-1} Cd	50 µmol L^{-1} Cd	100 µmol L^{-1} Cd	0 µmol L^{-1} Cd	50 µmol L^{-1} Cd	100 µmol L^{-1} Cd	0 µmol L^{-1} Cd	50 µmol L^{-1} Cd	100 µmol L^{-1} Cd
14:0	12.7 ± 3.3	9.8 ± 0.5	10.7 ± 0.4	7.1 ± 0.8	6.0 ± 0.7 *	6.9 ± 0.3	9.2 ± 0.9	7.4 ± 0.3	8.1 ± 0.7
16:0	206.6 ± 72.6	165.5 ± 17.9	191.9 ± 8.0	180.1 ± 34.0	158.0 ± 28.8	180.3 ± 17.7	175.8 ± 21.4	148.2 ± 21.7	166.4 ± 17.3
18:0	129.3 ± 39.8	120.4 ± 12.3	141.4 ± 4.7	132.2 ± 20.1	123.3 ± 19.3	140.7 ± 14.2	109.7 ± 18.2	99.5 ± 18.9	111.6 ± 10.3
Total SFA	**348.5 ± 115.6**	**295.7 ± 30.1**	**344.0 ± 11.7**	**319.4 ± 54.9**	**287.3 ± 48.7**	**327.9 ± 31.7**	**294.8 ± 40.0**	**255.2 ± 40.4**	**286.1 ± 28.0**
16:1n-7	11.6 ± 3.5	9.5 ± 1.1	10.5 ± 1.1	0.0 ± 0.0 *	0.0 ± 0.0 *	0.0 ± 0.0 *	5.5 ± 0.3	4.6 ± 0.5 (*)	5.6 ± 0.6
18:1n-7	27.5 ± 6.9	24.7 ± 2.2	28.6 ± 3.4	13.2 ± 0.9 (*)	10.7 ± 1.3 *	12.7 ± 0.5 *	17.0 ± 1.0	14.4 ± 1.3 (*)	16.7 ± 1.8
18:1n-9	232.4 ± 42.9	216.1 ± 18.0	248.2 ± 15.1	67.3 ± 6.2 *	59.9 ± 7.0 *	72.7 ± 5.2 *	91.5 ± 5.4 *	76.9 ± 6.9 *	93.3 ± 9.8 *
Total MUFA	**271.5 ± 53.0**	**250.3 ± 20.5**	**287.2 ± 19.4**	**80.5 ± 7.1 ***	**70.6 ± 8.3 ***	**85.4 ± 5.7 ***	**114.1 ± 6.7 ***	**95.9 ± 8.7 ***	**115.6 ± 12.1 ***
ALA 18:3n-3	0.0 ± 0.0	0.0 ± 0.0	0.0 ± 0.0	0.0 ± 0.0	0.0 ± 0.0	0.0 ± 0.0	0.0 ± 0.0	0.0 ± 0.0	0.0 ± 0.0
18:4n-3	0.0 ± 0.0	0.0 ± 0.0	0.0 ± 0.0	0.0 ± 0.0	0.0 ± 0.0	0.0 ± 0.0	0.0 ± 0.0	0.0 ± 0.0	0.0 ± 0.0
20:3n-3	0.0 ± 0.0	0.0 ± 0.0	0.0 ± 0.0	0.0 ± 0.0	0.0 ± 0.0	0.0 ± 0.0	0.0 ± 0.0	0.0 ± 0.0	0.0 ± 0.0
20:4n-3	0.0 ± 0.0	0.0 ± 0.0	0.0 ± 0.0	0.0 ± 0.0	0.0 ± 0.0	0.0 ± 0.0	0.0 ± 0.0	0.0 ± 0.0	0.0 ± 0.0
EPA 20:5n-3	8.2 ± 1.1	9.4 ± 0.6	10.4 ± 0.5	3.9 ± 0.7 (*)	4.1 ± 1.3 (*)	5.3 ± 0.4 (*)	0.0 ± 0.0 *	0.0 ± 0.0 *	0.0 ± 0.0 *
22:5n-3	9.4 ± 1.3	9.0 ± 0.9	10.2 ± 0.5	7.2 ± 1.2	6.0 ± 1.1	6.6 ± 0.6	7.5 ± 0.7	5.7 ± 0.5	6.4 ± 0.8
22:6n-3	14.6 ± 2.4	13.6 ± 1.6	17.9 ± 3.1	10.0 ± 2.0	8.8 ± 1.4	9.9 ± 0.9	10.6 ± 3.5	5.4 ± 0.4	5.9 ± 0.5 *
Total n-3 PUFA	**32.2 ± 4.2**	**32.0 ± 3.1**	**38.5 ± 3.8**	**21.1 ± 2.5**	**18.8 ± 3.7**	**21.7 ± 1.9**	**18.0 ± 4.0 (*)**	**11.1 ± 0.8 ***	**12.3 ± 1.2 ***
LA 18:2n-6	19.3 ± 3.9	18.4 ± 2.5	20.9 ± 1.8	**282.3 ± 45.8 ***	**239.2 ± 46.9 ***	**272.5 ± 29.7 ***	9.6 ± 1.0	7.8 ± 0.8 *	9.5 ± 1.3
18:3n-6	4.1 ± 0.8	4.1 ± 0.3	4.6 ± 0.7	47.6 ± 2.4 *	41.1 ± 4.0 *	48.9 ± 2.5 *	4.7 ± 0.3	4.1 ± 0.3	5.2 ± 0.3
20:2n-6	0.0 ± 0.0	0.0 ± 0.0	0.0 ± 0.0	12.6 ± 2.2 *	10.3 ± 2.1 *	11.3 ± 0.9 *	0.0 ± 0.0	0.0 ± 0.0	0.0 ± 0.0
20:3n-6	12.8 ± 2.0	12.4 ± 1.0	14.0 ± 0.7	26.4 ± 2.4 *	20.0 ± 2.5	22.2 ± 0.9	12.9 ± 0.6	10.5 ± 0.7	11.6 ± 1.0
AA 20:4n-6	20.6 ± 3.4	20.2 ± 2.0	23.0 ± 1.3	20.5 ± 1.8	16.9 ± 2.1	19.2 ± 1.3	**184.9 ± 18.6 ***	**155.4 ± 15.4 ***	**179.3 ± 23.5 ***
22:4n-6	0.0 ± 0.0	0.0 ± 0.0	0.0 ± 0.0	0.0 ± 0.0	0.0 ± 0.0	0.0 ± 0.0	71.7 ± 4.1 *	56.0 ± 3.2 *	62.1 ± 4.2 *
Total n-6 PUFA	**56.8 ± 10.1**	**55.1 ± 5.6**	**62.6 ± 4.2**	**389.3 ± 54.6 ***	**327.6 ± 57.5 ***	**374.1 ± 34.8 ***	**283.9 ± 23.7 ***	**233.8 ± 19.3 ***	**267.8 ± 29.0 ***
Total PUFA	**89.0 ± 14.2**	**87.1 ± 8.6**	**101.1 ± 7.7**	**410.4 ± 57.1 ***	**346.4 ± 61.3 ***	**395.8 ± 36.6 ***	**301.9 ± 25.5 ***	**244.9 ± 20.2 ***	**280.1 ± 30.2 ***
Total	**709.0 ± 179.7**	**633.2 ± 55.7**	**732.3 ± 36.4**	**810.3 ± 119.1**	**704.3 ± 113.7**	**809.2 ± 65.6**	**710.7 ± 70.7**	**596.0 ± 65.9**	**681.8 ± 69.6**
n-3/n-6 ratio	**0.58 ± 0.04**	**0.58 ± 0.00**	**0.62 ± 0.03**	**0.06 ± 0.01 ***	**0.06 ± 0.00 ***	**0.06 ± 0.00 ***	**0.06 ± 0.01 ***	**0.05 ± 0.00 ***	**0.05 ± 0.00 ***

Data are expressed as means ± standard error of mean (n = 3). For each level of Cd exposure, stars indicate significant differences between control and PUFA-enriched conditions ($p < 0.05$) while stars into brackets indicate similar trends but without significance ($0.05 < p < 0.1$). Abbreviations used: AA, arachidonic acid; Cd, cadmium; LA, linoleic acid; MUFA, monounsaturated fatty acid; PUFA, polyunsaturated fatty acid; SFA, saturated fatty acid.

L^{-1} Cd. On the other hand, LA enrichment had no impact on any of the cell viability indicators whatever the Cd concentration (Fig. 2).

3.6. PUFA has no impact on Cd burden

RTL-W1 dose-dependently accumulated Cd, irrespective of the PUFA enrichment strategy (Fig. 3). The total Cd burden was not significantly different between PUFA-enriched cells and control cells (Fig. 3).

3.7. PUFA and Cd modulate the expression of genes and the proteomic landscape

Raw data for proteomic analyses are available in Table A1 in Supplementary material.

3.7.1. Fatty acid metabolism

The expression level of the *ELOVL2* gene was below quantification limit for all experimental conditions (not shown). In the absence of Cd challenge, PUFA enrichments significantly increased *FATP1* and *CPT1* gene expression levels, while having no significant impact on the expression level of the other fatty acid metabolism genes analysed (*FASN*, *FADS2* and *ELOVL5*) (Fig. 4). At the protein expression level, ALA, EPA and AA enrichments significantly downregulated the fatty acid binding protein 7 (FABP7), a protein involved in fatty acid uptake, transport and metabolism. This effect was unaffected by Cd exposure (proteomic analyses, Table 6).

Cd had no significant impact on *FATP1*, *CPT1* and *ELOVL5* gene expression (Fig. 4). Cd tended to decrease the *FASN* gene expression in PUFA-enriched cells (especially in ALA- and LA-enriched cells), while the *FASN* gene expression remained constant under Cd exposure in control cells (Fig. 4). As a result, a trend for lower *FASN* gene expression was observed in PUFA-enriched cells (especially ALA-, EPA- and LA-

Table 5
Fatty acid composition of RTL-W1 cell neutral lipids after one week culture in a growth medium supplemented in AA (50 µmol L^{-1}) and a subsequent challenge with Cd (0, 50 or 100 µmol L^{-1}) during 24 h in a medium deprived of fatty acid (µmol g^{-1} protein).

Fatty acid	0 µmol L^{-1} Cd	50 µmol L^{-1} Cd	100 µmol L^{-1} Cd
16:0	21.2 ± 1.6	22.9 ± 7.3	14.8 ± 1.1
18:0	28.9 ± 5.0	28.5 ± 8.7	21.3 ± 4.9
Total SFA	**50.2 ± 6.4**	**51.4 ± 15.9**	**36.1 ± 6.0**
18:1n-9	3.5 ± 0.5	6.0 ± 3.4	4.3 ± 0.5
Total MUFA	**3.5 ± 0.5**	**6.0 ± 3.4**	**4.3 ± 0.5**
Total PUFA n-3	**0.0 ± 0.0**	**0.0 ± 0.0**	**0.0 ± 0.0**
AA 20:4n-6	**6.0 ± 0.5 (a)**	**7.4 ± 1.6 (ab)**	**16.3 ± 4.6 (b)**
22:4n-6	2.6 ± 0.0 [a]	2.6 ± 0.3 [a]	5.0 ± 0.8 [b]
Total PUFA n-6	**8.6 ± 0.5 [a]**	**10.0 ± 1.8 ab(a)**	**21.3 ± 5.4 [b]**
Total PUFA	**8.6 ± 0.5 [a]**	**10.0 ± 1.8 ab(a)**	**21.3 ± 5.4 [b]**
Total	**62.3 ± 7.0**	**67.4 ± 20.9**	**61.7 ± 11.6**

Data are expressed as means ± standard error of mean (n = 3). Letters indicate significant impact of the Cd exposure level, with levels not connected to the same letter being significantly different from each other, ($p < 0.05$) while letters into brackets indicate similar trends but without significance ($0.05 < p < 0.1$). Abbreviations used: AA, arachidonic acid; Cd, cadmium; MUFA, monounsaturated fatty acid; PUFA, polyunsaturated fatty acid; SFA, saturated fatty acid.

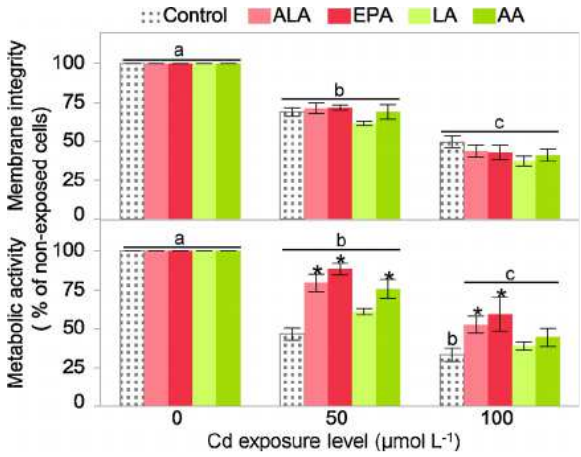

Fig. 2. Membrane integrity (up) and metabolic activity (down) of RTL-W1 cells after one week culture in a growth medium supplemented or not (control) in a specific PUFA (50 µmol L^{-1} ALA, EPA, LA or AA) and a subsequent challenge with Cd (0, 50 or 100 µmol L^{-1}) during 24 h in a medium deprived of fatty acid. Data are expressed as means ± standard error of mean (n = 6). For each level of Cd exposure, stars indicate significant differences between control and PUFA-enriched conditions ($p < 0.05$). For each PUFA enrichment strategy, letters indicate significant impact of the Cd exposure level, with levels not connected to the same letter being significantly different from each other ($p < 0.05$). Abbreviations used: AA, arachidonic acid; ALA, alpha-linolenic acid; Cd, cadmium; EPA, eicosapentaenoic acid; LA, linoleic acid, PUFA, polyunsaturated fatty acid.

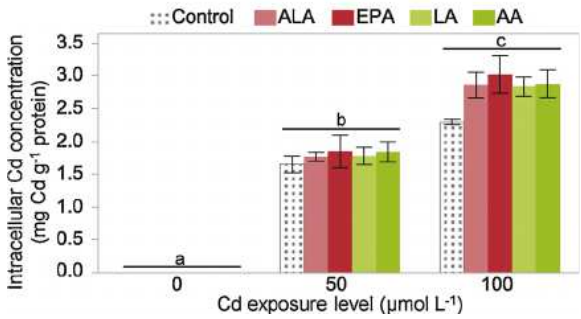

Fig. 3. Intracellular Cd concentration in RTL-W1 cells after one week culture in a growth medium supplemented or not (control) in a specific PUFA (50 µmol L^{-1} ALA, EPA, LA or AA) and a subsequent challenge with Cd (0, 50 or 100 µmol L^{-1}) during 24 h in a medium deprived of fatty acid. Data are expressed as means ± standard error of mean (n = 4). For each PUFA enrichment strategy, letters indicate significant impact of the Cd exposure level ($p < 0.05$). For more details, refer to the legend of Fig. 2 PUFA enrichments had no significant impact on the intracellular Cd concentration. Abbreviations used: AA, arachidonic acid; ALA, alpha-linolenic acid; Cd, cadmium; EPA, eicosapentaenoic acid; LA, linoleic acid, PUFA, polyunsaturated fatty acid.

enriched cells) exposed to 100 µmol L^{-1} Cd as compared to control cells exposed to the same Cd dose (Fig. 4). Besides, Cd tended to downregulate the *FADS2* gene in PUFA-enriched cells (especially in EPA-enriched cells) (Fig. 4).

3.7.2. PUFA-derived signalling

In the absence of Cd challenge, EPA enrichment slightly, yet significantly, upregulated the *cPLA2* gene expression (1.4-fold) while the other PUFA enrichments had no impact (Fig. 5). The expression level the *COX2* gene was significantly lower (4-fold) in AA-enriched cells than in control cells. A similar trend, but of lower magnitude, was observed in EPA-enriched cells. ALA and LA enrichments had no impact on the *COX2* gene expression level (Fig. 5). AA enrichment tended to decrease *ALOX5* gene expression level while the other PUFA enrichments had no impact (Fig. 5).

Cd significantly upregulated the *cPLA2* gene expression in control cells (4.5-fold increase at the highest dose tested) (Fig. 5). The *cPLA2* gene expression level was significantly lower in ALA-, EPA- and AA-enriched cells exposed to 100 µmol L^{-1} Cd than in control cells challenged with the same Cd dose (Fig. 5). The *COX2* gene expression was significantly decreased by Cd in ALA- and LA-enriched cells (Fig. 5). Similar downregulations, not significant though, were observed in EPA-enriched cells (at both Cd doses) and in control cells (at the lowest Cd dose tested only) while Cd had no impact on the *COX2* gene expression level in AA-enriched cells (Fig. 5). Finally, Cd had no impact on the *ALOX5* gene expression level, regardless of the PUFA enrichment strategy (Fig. 5).

3.7.3. Stress response

The expression level of the *HSP70b* gene was below quantification limit for all treatments (not shown). In the absence of Cd challenge, RTL-W1 cells did not express the *MTa* gene at detectable levels while they markedly expressed the *MTb* isoform (Fig. 6). The basal expression level of the latter gene was not influenced by PUFA enrichment strategies (Fig. 6). PUFA enrichments did not impact the gene expression of *HSP70a*, *p53* or *CALR* (Fig. 6). ALA, LA and AA enrichments tended to downregulate the *BCLx* gene (Fig. 6). At the protein expression level, EPA enrichment tended to downregulate glutaredoxin-1. ALA and AA enrichments tended to downregulate S100-A1, a protein involved in many cellular functions, including calcium homeostasis, cytoskeleton dynamics and the inflammatory response. The observed downregulation of glutaredoxin-1 and protein S100-A1 disappeared after Cd exposure (50 µmol L^{-1}) (proteomic analyses, Table 6)

Cd significantly induced *MTa*, *HSP70a* and *MTb* gene expression levels while it decreased that of *BCLx* and had no significant impact on *p53* and *CALR* gene expression levels (Fig. 6). The upregulation of the *MTb* gene was less pronounced in PUFA-enriched cells and decreased with the Cd exposure level (Fig. 6). As a result, *MTb* gene expression level was significantly lower (or tended to be so) in ALA-, EPA- and AA-enriched cells exposed to 100 µmol L^{-1} Cd than in control cells exposed to the same Cd level (Fig. 6). The *MTa* gene expression followed a similar pattern, with a significantly lower expression level in AA-enriched cells exposed to 100 µmol L^{-1} Cd than in control cells (Fig. 6). At the protein expression level, Cd strongly upregulated several HSPs, namely HSP30 and two isoforms of HSP70. However, due to a high variability of response, the upregulation of one of the HSP70 isoforms was only significant in control cells, and the upregulation of HSP30 was not significant (only a trend was seen in control cells) (proteomic analyses, Table 6). Besides, ALA-enriched cells showed higher levels of an isoform of the antioxidant enzyme peroxiredoxin (predicted: peroxiredoxin-1, blast NCBI) when challenged with Cd (50 µmol L^{-1}), while no impact was observed in the absence of Cd (proteomic analyses, Table 6). A similar trend, but without significance, was observed in AA-enriched cells, while EPA enrichment had no impact on the production of this protein. Finally, in control and AA-enriched cells, Cd (50 µmol L^{-1}) significantly downregulated annexin-A1, a protein involved in trafficking and organisation of vesicles, exocytosis and endocytosis processes as well as in calcium ion channel formation (proteomic analyses, Table 6).

3.7.4. CYP20A1

In absence of Cd challenge, EPA and AA enrichments significantly increased the expression level of the *CYP20A1* gene, an orphan of the *CYP* family (Fig. 7).

Both doses of Cd repressed the *CYP20A1* gene expression level in EPA-enriched cells, whereas no significant impact of Cd on the *CYP20A1* expression level could be detected in control cells and cells enriched in other PUFAs (Fig. 7).

3.7.5. Cytoskeleton

At the protein expression level, PUFA enrichments influenced the abundance of some cytoskeletal intermediate filaments. In absence of Cd challenge, cytokeratin-18 level was significantly higher in ALA- and

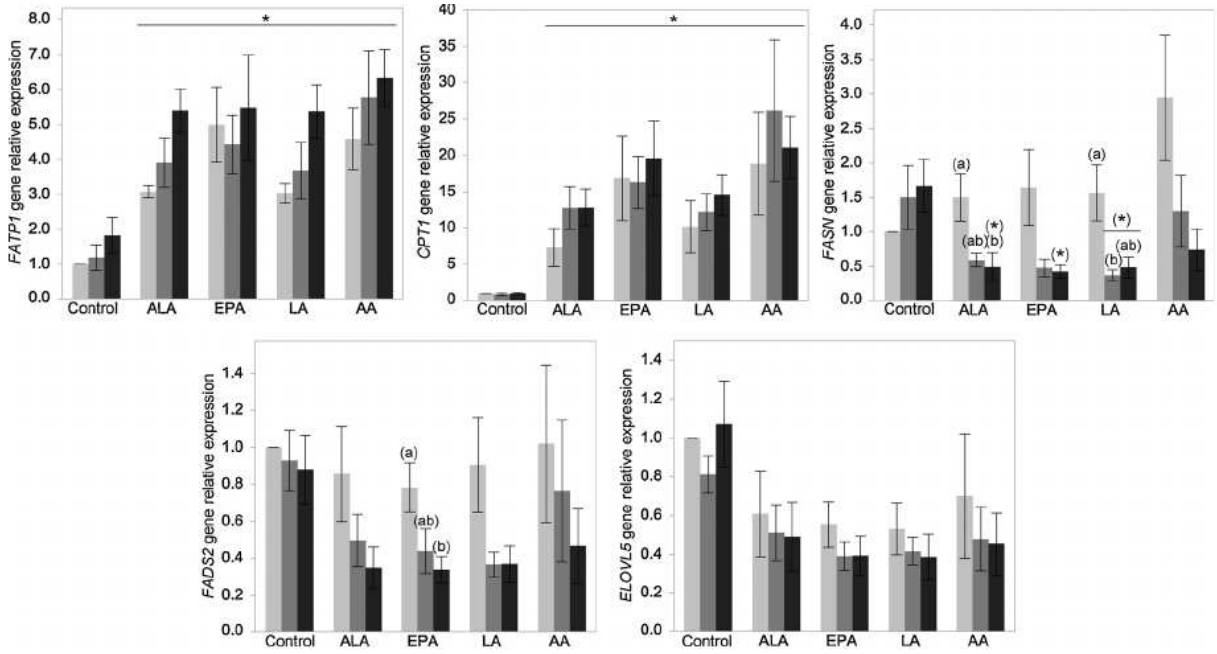

Fig. 4. Relative expression of genes involved in lipid metabolism in RTL-W1 cells after one week culture in a growth medium supplemented or not (control) in a specific PUFA (50 µmol L^{-1} ALA, EPA, LA or AA) and a subsequent challenge with Cd (0 µmol L^{-1} in light grey, 50 µmol L^{-1} in grey or 100 µmol L^{-1} in dark grey) during 24 h in a medium deprived of fatty acid. Data are expressed as means ± standard error of mean (n = 4). For each level of Cd exposure, stars indicate significant differences between control and PUFA-enriched conditions ($p < 0.05$), while stars intro brackets indicate similar trends but without significance ($0.05 < p < 0.1$). For each PUFA enrichment strategy, letters indicate significant impact of the Cd dose, with levels not connected to the same letter being significantly different from each other ($p < 0.05$), while letters intro brackets indicate similar trends but without significance ($0.05 < p < 0.1$). Abbreviations used: AA, arachidonic acid; ALA, alpha-linolenic acid; Cd, cadmium; *CPT1*, carnitine palmitoyl transferase 1; *ELOVL5*, fatty acid elongase 5; EPA, eicosapentaenoic acid; *FADS2*, fatty acid desaturase 2; *FASN*, fatty acid synthase; *FATP1*, fatty acid transport protein 1; LA, linoleic acid; PUFA, polyunsaturated fatty acid.

AA-enriched cells than in control cells. Besides, AA-enriched cells contained a significantly higher amount of intermediate filament protein ON3 than control cells. Finally, ALA, AA and EPA enrichments slightly reduced myosin-9 level (significant for AA and EPA enrichments). These PUFA-derived regulations disappeared after Cd exposure (50 µmol L^{-1}) (proteomic analyses, Table 6).

3.7.6. Glucose metabolism

In absence of Cd challenge, AA enrichment significantly upregulated pyruvate kinase expression (proteomic analyses, Table 6), a protein involved in glucose metabolism, while ALA and EPA enrichment had no impact. This upregulation was not observed under Cd exposure (50 µmol L^{-1}).

Table 6
Differentially expressed proteins in RTL-W1 cells after one week culture in a growth medium supplemented or not (control) in a specific PUFA (50 µmol L^{-1} ALA, EPA or AA) and a subsequent challenge with Cd (0 or 50 µmol L^{-1}) during 24 h in a medium deprived of fatty acid.

Proteins	PUFA impact in absence of Cd			PUFA impact in presence of Cd			Cd impact			
	ALA0/CT0	EPA0/CT0	AA0/CT0	ALA50/CT50	EPA50/CT50	AA50/CT50	CT50/CT0	ALA50/ALA0	EPA50/EPA0	AA50/AA0
Glucose metabolism										
Pyruvate kinase	1.08	1.14	1.27 *	0.98	1.03	1.09	1.00	0.91	0.95	0.90
Fatty acid metabolism										
Fatty acid binding protein 7	0.57 *	0.52 *	0.59 *	0.62 *	0.53 *	0.64 *	1.08	1.05	0.87	0.96
Stress response										
Annexin-A1	0.93	1.00	1.05	1.01	1.03	0.96	0.73 (*)	0.86	0.82	0.67 (*)
Glutaredoxin-1	0.82	0.69 (*)	0.80	0.77	0.92	0.93	1.11	0.91	1.06	1.11
Heat shock protein 30	0.66	0.76	0.67	1.33	1.09	1.31	4.07 (*)	5.16	3.26	5.00
Heat shock protein 70-1	1.00	0.88	1.25	1.03	0.94	0.91	3.73 *	1.48 *	1.35 *	1.32 *
Heat shock protein 70-2	0.82	1.09	1.11	1.08	1.04	0.95	5.92 *	4.99	3.82	3.81
Peroxiredoxin-1	1.19	1.03	1.07	1.39 *	0.97	1.26 (*)	0.90	1.09	0.89	1.12
Protein S100-A1	0.56 (*)	0.66	0.62 (*)	0.90	1.37	1.32	1.11	1.00	1.30	1.16
Cytoskeleton										
Cytokeratin-18	1.37 *	1.32	1.38 *	0.93	0.89	0.98	1.20	0.97	0.92	1.14
Intermediate filament protein ON3	1.26	1.29	1.39 *	1.01	1.00	1.07	1.16	0.96	0.94	0.96
Myosin-9	0.88 (*)	0.83 *	0.78 *	0.92	0.92	0.90	1.03	1.04	0.96	1.03

Data are expressed as mean ratios (n = 3). Stars indicate significant upregulation (green) or downregulation (red) by PUFAs or Cd (i.e. ratios significantly different from 1, weighed z-scores, $p < 0.05$) while stars into brackets indicate similar trends but without significance ($0.05 < p < 0.1$). Desciption (Oncorhynchus_peptide database): Annexin-A1, GSONMP00063408001; Cytokeratin-18, GSONMP00010164001; Fatty acid binding protein 7, GSONMP00072181001; Glutaredoxin-1, GSONMP00066197001; Heat shock protein 30, GSONMP00081507001; Heat shock protein 70-1, GSONMP00064818001; Heat shock protein 70-2, GSONMP00020100001; Intermediate filament protein ON3, GSONMP00040665001; Myosin-9, GSONMP00017263001; Peroxiredoxin-1, GSONMP00041410001; Protein S100-A1, GSONMP00014770001; ; Pyruvate kinase, GSONMP00052888001;. Abbreviations used: AA, arachidonic acid; ALA, alpha-linolenic acid; Cd, cadmium; CT, control; EPA, eicosapentaenoic acid; LA, linoleic acid, PUFA(s), polyunsaturated fatty acid(s).

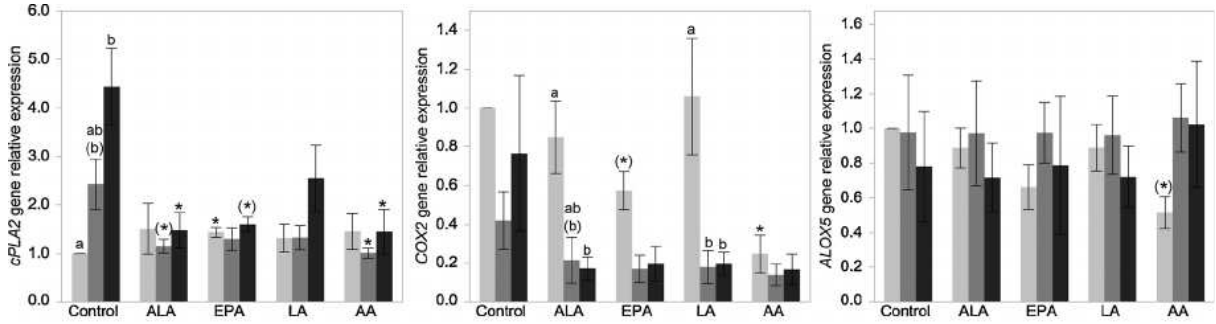

Fig. 5. Relative expression of genes involved in PUFA-derived signalling metabolism in RTL-W1 cells after one week culture in a growth medium supplemented or not (control) in a specific PUFA (50 µM ALA, EPA, LA or AA) and a subsequent challenge with Cd (0 µmol L^{-1} in light grey, 50 µmol L^{-1} in grey or 100 µmol L^{-1} in dark grey) during 24 h in a medium deprived of fatty acid. Stars and letters indicate significant impacts of PUFA enrichment and Cd exposure, respectively. For more details, refer to the legend of Fig. 4. Abbreviations used: AA, arachidonic acid; ALA, alpha-linolenic acid; *ALOX5*, arachidonate 5-lipoxygenase; Cd, cadmium; *cPLA2*, cytosolic phospholipase A2; *COX2*, cyclooxygenase 2, EPA, eicosapentaenoic acid; LA, linoleic acid; PUFA, polyunsaturated fatty acid.

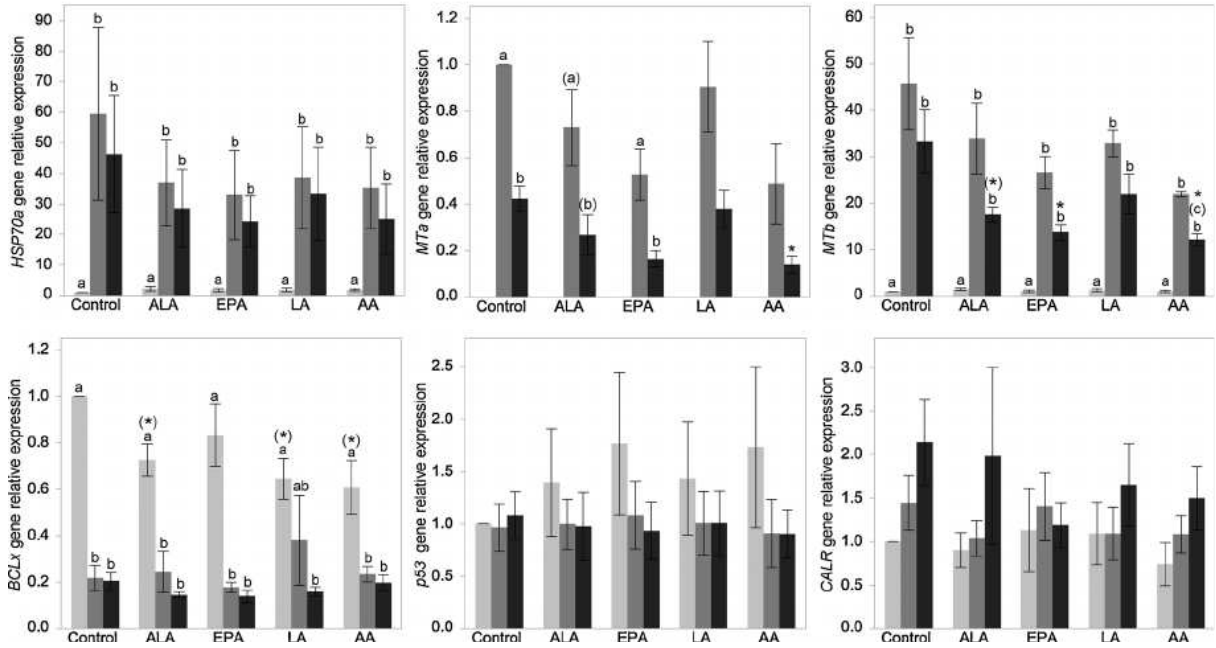

Fig. 6. Relative expression of genes involved in stress response metabolism in RTL-W1 cells after one week culture in a growth medium supplemented or not (control) in a specific PUFA (50 µM ALA, EPA, LA or AA) and a subsequent challenge with Cd (0 µmol L^{-1} in light grey, 50 µmol L^{-1} in grey or 100 µmol L^{-1} in dark grey) during 24 h in a medium deprived of fatty acid. Stars and letters indicate significant impacts of PUFA enrichment and Cd exposure, respectively. For more details, refer to the legend of Fig. 4. Abbreviations used: AA, arachidonic acid; ALA, alpha-linolenic acid; *BCLx*, apoptosis regulator BCL2-Like1; *CALR*, calreticulin; EPA, eicosapentaenoic acid; *HSP70a*, heat shock protein 70a; LA, linoleic acid; *MTa*, metallothionein a; *MTb*, metallothionein b; *p53*, tumor protein 53; PUFA, polyunsaturated fatty acid.

4. Discussion

The present study aimed at investigating the interactions between PUFAs and Cd at the molecular level. Globally, our results indicate that PUFAs strongly influenced fatty acid homeostasis and metabolism while Cd moderately impacted these parameters. They further indicated that some PUFAs modulated the sensitivity of rainbow trout liver cells to Cd. This protective effect could not be ascribed to a differential Cd accumulation. Rather, it is suggested that modulation of intracellular parameters was responsible for the increased tolerance to Cd.

4.1. Impact of PUFA on fatty acid homeostasis and metabolism in RTL-W1 cells

As previously observed (Ferain et al., 2016), RTL-W1 cells supplemented with single PUFAs incorporated these compounds as well as some biotransformation products mainly in their phospholipids, while keeping the total cellular fatty acid content stable. This indicates that the fatty acid profile modulation occurred either through the replacement of some fatty acids (mainly 18:1n-9) in pre-existing lipids or thanks to the lipid turnover process rather than through supplementary lipid accumulation, as previously pointed out (Ferain et al., 2016). As a result, RTL-W1 cells grown in a culture medium supplemented with a specific PUFA were not only richer in PUFAs but also lower in MUFAs than the control cells, as previously described (Ferain et al., 2016). The major incorporation of the absorbed PUFAs in the cellular phospholipids emphasises once more the preponderant role of PUFAs as structural components of biological membranes (Tocher, 2003).

Fatty acids are absorbed by cells through either a passive mechanism or by transmembrane proteins, such as FATP1 (Frohnert and Bernlohr, 2000; Zhou et al., 2010). The upregulation of *FATP1* gene detected with the PUFA treatments may be a cellular response aiming at increasing the efficiency of the PUFA uptake, which may have been driven either by the high PUFA concentration in the growth medium or

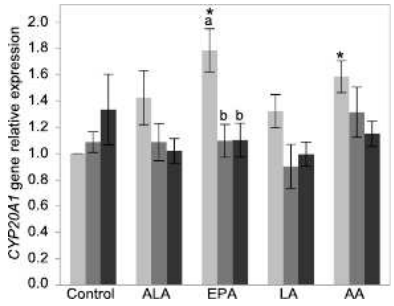

Fig. 7. Relative expression of *CYP20A1* gene metabolism in RTL-W1 cells after one week culture in a growth media supplemented or not (control) in a specific PUFA (50 µmol L^{-1} ALA, EPA, LA or AA) and a subsequent challenge with Cd (0 µM in light grey, 50 µmol L^{-1} in grey or 100 µmol L^{-1} in dark grey) during 24 h in a medium deprived of fatty acid. Stars and letters indicate significant impacts of PUFA enrichment and Cd exposure, respectively. For more details, refer to the legend of Fig. 4. Abbreviations used: AA, arachidonic acid; ALA, alpha-linolenic acid; Cd, cadmium; *CYP20A1*, cytochrome P450 20A1; EPA, eicosapentaenoic acid; LA, linoleic acid; PUFA, polyunsaturated fatty acid.

by an increased mitochondrial β-oxidation rate. Indeed, it has been suggested that the metabolic demand for fatty acids and not the substrate availability is the driving force for cellular fatty acid uptake (Mashek and Coleman, 2006). The upregulation of *CPT1* gene supports this view since the enzyme encoded by this gene catalyses the complexation of activated fatty acids with carnitine, a crucial step for their translocation into mitochondria for β-oxidation (Fig. 1) (Leaver et al., 2008). The intracellular transport of free fatty acids is facilitated by proteins called fatty acid binding proteins as they bind the hydrophobic fatty acids (Leaver et al., 2008). Contrary to expectations, PUFA treatments decreased the level of FABP-7, a fatty acid binding protein isoform. Other isoforms may thus preponderantly ensure cytosolic transport of fatty acids in RTL-W1 cells.

Rainbow trout, like other salmonids, have high fatty acid biotransformation abilities and can efficiently produce DHA and AA from 18 carbon precursors (ALA and LA) (Tocher, 2003). These biotransformation steps (Fig. 1), mainly occurring in the liver, are catalysed by elongases and desaturases. These enzymes are encoded by the *ELOVL2*, *ELOVL5* and *FADS2* genes (Leaver et al., 2008). In line with previous reports (Ferain et al., 2016; Mellery et al., 2017), RTL-W1 cells were unable to produce DHA from ALA or from EPA, and AA from LA. Instead, an accumulation of intermediary elongation and desaturation (Δ5 and Δ6) products immediately downstream of the given PUFAs in the biotransformation pathway was observed, as previously described (Ferain et al., 2016; Mellery et al., 2017). The absence of *ELOVL2* expression in RTL-W1 cells under the present experimental conditions might explain their inability to generate DHA, as previously suggested (Ferain et al., 2018).

4.2. Impact of Cd on fatty acid homeostasis and metabolism in RTL-W1 cells

The fatty acid profile of fish tissue is influenced by environmental factors, including pollution by metals (Fadhlaoui and Couture, 2016; Filimonova et al., 2016; Konar et al., 2010). Nevertheless, very few works addressed the specific impact of Cd on the fatty acid composition of cellular lipid classes. A previous study on rat hepatocytes showed that a sub-lethal dose of Cd increased the relative parts of 16:0 and 18:0 while decreasing that of AA in neutral lipids (Kudo and Waku, 1996). In the present study, Cd neither impacted on the fatty acid composition of cellular lipids (neutral lipids and phospholipids), nor the expression of genes involved in fatty acid metabolism in control cells. On the other hand, Cd modulated these parameters in PUFA-enriched cells. In particular Cd significantly increased (2.5-fold) the incorporation of AA in neutral lipids of AA-enriched cells at the expense of other fatty acids (mainly SFAs). Since Cd exposure was carried out in a fatty acid free medium and the n-6 PUFA level remained constant in phospholipids under Cd exposure, n-6 PUFAs incorporated into neutral lipids in response to Cd exposure likely originated from the cellular free fatty acid pool. Further investigation is, however, needed to validate this hypothesis as the free fatty acid fraction was not analysed in the present experiment. Besides, in the present study, DHA phospholipid level was significantly lower in AA-enriched cells than in control cells after exposure to the highest dose of Cd, while there was no difference in absence of Cd challenge. This resulted from two opposite trends (not significant), i.e. an increase (vs a decrease) of DHA level following Cd exposure in control-cells (vs in AA-enriched cells). The biological relevance of these changes remains unclear.

Previous studies have shown that Cd can modulate the expression of genes involved in fatty acid metabolism. However, the reported effects are highly variable and depend on the exposure characteristics (concentration, duration) (Koskinen et al., 2004), on the tissue targeted (Chen et al., 2013; Fadhlaoui et al., 2018), on environmental conditions (water temperature during fish growth) (Fadhlaoui et al., 2018). For instance, a Cd challenge of high intensity (0.5 mg L^{-1}, 96 h) downregulated genes related to biosynthesis of fatty acids in rainbow trout while a Cd challenge of a lower intensity (0.05 or 0.025 mg L^{-1}, 24 h) upregulated these genes (Koskinen et al., 2004). In the present study, Cd tended to downregulate *FASN* (about 3- to 4-fold, not significant) and *FADS2* (about 2- to 2.5-fold, not significant) in PUFA-enriched cells while Cd did not affect these genes in control cells. Downregulations of these genes by Cd were also reported in primary cultures of Atlantic salmon hepatocytes (Olsvik et al., 2016) and in liver of rats (Madejczyk et al., 2015). All together, these data suggest that Cd might negatively affect salmonid ability to synthesize EPA and DHA, thereby decreasing the nutritional value of its flesh. Further studies are needed to identify the critical conditions in which Cd really alters PUFA biosynthesis in fish.

4.3. Impact of PUFA on Cd sensitivity

At both Cd doses tested, ALA- and EPA-enriched cells were more metabolically active than the control cells, while LA enrichment had no impact. This cytoprotection exerted by ALA and EPA confirmed our previous observation with the same cell line (Ferain et al., 2016). Similarly, n-3 PUFAs (EPA and DHA mix) increased cell tolerance to 24 h and 48 h Cd challenge in Hep G2 cells (Linhartova and Sampels, 2015). Still, in contrast to our previous observations, AA-enrichment also increased cell tolerance to 50 µmol L^{-1} Cd but not to 100 µmol L^{-1} Cd, in the present study. This divergence could most probably reflect differences in the experimental procedures. Indeed, the protective effect of PUFAs toward Cd toxicity was herein evaluated at two discrete Cd concentrations, while it was assessed by EC50 calculation through modelling toxicity data in our previous study (Ferain et al., 2016).

In the present study, we explore two hypotheses that may explain the cytoprotection exerted by specific PUFAs. PUFAs might (i) decrease Cd cellular uptake and/or (ii) modulate intracellular parameters increasing the cell tolerance to the damages induced by Cd (Ferain et al., 2016).

- Cd burden was not influenced by PUFA enrichment

Depending on their number of carbons and unsaturation level, PUFAs confer different physicochemical properties to the biological membranes (fluidity, permeability), which can affect both active and passive transports of solutes (Arts and Kohler, 2009; Tillman and Cascio, 2003). However, in the present study, cytoprotection conferred by ALA, EPA and AA was not associated with a decrease in intracellular Cd concentration. Interestingly, n-3 PUFAs (EPA and DHA mixture) increased Hep G2 cells tolerance to Cd (5 µmol L^{-1}, 24 h) while they significantly increased Cd intracellular burden (Linhartova and

Sampels, 2015). Overall, these results highlight that PUFAs do not protect cells against Cd toxicity by decreasing Cd burden. Nevertheless, one cannot exclude that PUFA enrichments could influence Cd intracellular distribution, thereby modulating Cd toxicity. In cells, Cd can indeed be found in five separate pools: (i) metallothionein-like proteins, (ii) metal-rich granules, (iii) cellular debris (membrane), (iv) heat sensitive proteins (e.g. enzymes) and (v) organelles (e.g. nucleus, mitochondria) (Wang and Rainbow, 2006). The two latter pools represent the metal sensitive fraction, while the two former ones represent the detoxification fraction (Wallace et al., 2003; Wang and Rainbow, 2006). Whether individual PUFAs may modulate the repartition of Cd between these two fractions and thereby affect the fate of cells (survival or death) is currently unknown but worth investigating.

- PUFAs modulated transcriptomic and genetic responses to Cd

MTs are cysteine-rich proteins that scavenge metal ions and reactive oxygen species (Fig. 1). They can thus reduce cellular availability of toxic metals such as Cd. In accordance with previous studies in mammals (Cartularo et al., 2015; Go et al., 2014) and fish (Chen et al., 2014; Qiang et al., 2018; Walker et al., 2008), Cd strongly induced the expression of two isoforms of *MT*, i.e. *MTa* and *MTb*, in RTL-W1 cells. Interestingly, cytoprotection conferred by ALA, EPA and AA seemed to go along with a lower induction of *MT* genes. Since Cd intracellular concentrations were not influenced by PUFA enrichment, such a decrease in *MT* expression is likely not linked to a decrease in Cd level but rather might indicate a reduction of intracellular levels of free metal ions or ROS by other mechanisms such as subcellular Cd partitioning.

Cd is known to induce oxidative stress in liver cells (Jamwal et al., 2016; Linhartova et al., 2016; Matović et al., 2015; Wang et al., 2014). Interestingly, the supplementation with a mixture of EPA and DHA protected Hep G2 cells against the Cd-induced oxidative damages to lipids and proteins (Linhartova et al., 2016). This effect was associated with a lower level of superoxide dismutase activity (Linhartova et al., 2016). This suggests that PUFA-derived cytoprotection could, at least partly, be explained by a reduction of the oxidative stress induced by Cd. Likewise, in the present study, interactive effects between cytoprotective PUFAs (EPA, ALA and AA) and the levels of antioxidant enzymes were observed either in the absence (EPA) or in the presence (ALA and AA) of Cd. On the one hand, the lower level of the antioxidant enzyme glutaredoxin-1 in EPA-enriched cells in the absence of Cd challenge as compared to control cells, pleads for lower basal ROS production in cells enriched in this PUFA. This could result from a direct impact of EPA on the mitochondrial electron transport chain, i.e. decrease of electron leakage and hydrogen peroxide generation through modulations of the activities of the mitochondrial complexes I, III and IV, as previously demonstrated in mice (Hagopian et al., 2010). On the other hand, we observed that the ALA-enriched cells had significantly higher protein levels of peroxiredoxin-1 under Cd stress than control cells, while the basal level of this antioxidant enzyme was similar in the absence of Cd challenge. A similar trend was observed in AA-enriched cells. Since peroxiredoxin-1 catalyses the reduction of hydrogen peroxide, peroxynitrite and organic hydroperoxides (Wood et al., 2003), the higher level of this antioxidant enzyme may have conferred a higher detoxification ability against Cd-induced ROS production in ALA- and AA-enriched cells. All together, these results reinforce the view that PUFAs are likely to increase cell tolerance and response to oxidative stress. This may counteract to some extent Cd toxicity.

Oxidative stress induced by Cd can damage lipids, DNA and proteins. HSPs play an important role in cell response to metal toxicity as these chaperone proteins refold damaged proteins and target the highly-damaged ones for degradation (Deane and Woo, 2011) (Fig. 1). In agreement with the literature (Deane and Woo, 2011; Lu et al., 2011; Mills and Gallagher, 2017), results from the present study highlight a strong induction of several HSPs at both transcriptomic and proteomic levels in RTL-W1 cells exposed to Cd. PUFA enrichments had no impact on this parameter, suggesting that the PUFA-derived cytoprotection observed in the present experiment is not linked to a differential expression of HSPs. As it is the case for proteins, cells possess mechanisms to repair DNA damages inflicted by oxidative stress. However, Cd has been reported to affect DNA repair mechanisms. Specific mechanisms are not well understood but the implication of p53, a transcription factor involved in the regulation of DNA repair and cell cycle arrest, has been suggested (Antoniali et al., 2015). In the present study, though, neither Cd nor PUFA enrichments influenced *p53* gene expression.

Cd is known to alter ion homeostasis, especially calcium homeostasis, which can lead to increased ROS production, mitochondrial membrane depolarisation and apoptosis (McGeer et al., 2011; Thévenod and Lee, 2013; Wang et al., 2014). In the present study, the level of annexin-A1, a multifunctional protein involved in calcium ion channel formation, was reduced by Cd exposure in control and AA-enriched cells. On the other hand, no impact of Cd could be detected on S100-A1, a calcium-binding protein, or on CALR, a calcium-dependent chaperone located in the endoplasmic reticulum (Fig. 1). However, in the absence of Cd challenge, ALA and AA enrichments influenced the level of S100-A1. Further research is needed to determine whether a reduced basal level of S100-A1 could contribute to the lower sensitivity to Cd observed in ALA- and AA-enriched cells.

As mentioned above, Cd toxicity is partly due to its capacity to trigger cell apoptosis through different mechanisms. Among these, the increase in ROS production, the rise in free cytosolic calcium or the modulation of anti- and pro-apoptotic members of BCL2 family (Morcillo et al., 2016; Olszowski et al., 2015; Thévenod and Lee, 2013; Wang et al., 2014). Here, Cd exposure strongly decreased the expression level of *BCLx* gene, an anti-apoptotic member of the BCL2 family (Fig. 1). However, none of the PUFA enrichments that protected RTL-W1 cells against Cd prevented *BCLx* gene decreased expression. This is in agreement with the previous report stating that EPA (300 µmol L^{-1}) had no impact on *BCLx* gene expression in ASK cells exposed to methylmercury (2.5 µmol L^{-1}, 48 h) although it reduced cell apoptosis (Nøstbakken et al., 2012). The reduction of metal-driven apoptosis by PUFA enrichments may result from other direct or indirect mechanisms such as a direct modulation of other members of the BCL2 family (e.g. pro-apoptotic Bax) or a differential modulation of calcium intracellular level by AA- or EPA-derived eicosanoids. Further studies are needed to better understand the mechanisms behind PUFA protective effect on metal-induced apoptosis.

Fatty acids with 20 and 22 carbons (such as AA, EPA, 20:3n-6 and DHA) are precursors of eicosanoids, protectins and resolvins (Kremmyda et al., 2011). These PUFA-derived bioactive molecules are modulators of several processes such as inflammation, ion transport and cellular redox status (Kremmyda et al., 2011). PUFAs are first released from the cellular membrane through the action of phospholipases (e.g. cPLA2), then oxidized into bioactive prostanoids, leukotrienes, protectins and resolvins by cyclooxygenases (e.g. COX2) and lipoxygenases (e.g. ALOX5) (Kremmyda et al., 2011) (Fig. 1). Cd has been shown to induce the eicosanoid cascade through notably upregulation of the *cPLA2* gene (Madejczyk et al., 2015; Miyahara et al., 2001). Likewise, Cd upregulated the *cPLA2* gene in control and LA-enriched cells in the present study (4.5- and 2-fold increase, significant in control cells). Together with the lower level annexin-A1, an inhibitor of cPLA2 (Parente and Solito, 2004), observed in control cells exposed to Cd, this upregulation of the *cPLA2* gene pleads for a high induction of the eicosanoid cascade by Cd in control cells. Interestingly, the *cPLA2* gene expression remained constant under Cd challenge in the PUFA-enriched cells that were more resistant to Cd, i.e. ALA, EPA- and AA-enriched cells. This suggests that PUFA-derived cytoprotection mechanism against Cd might include a repression of the eicosanoid cascade. This repression may, for instance, have been driven through the reduction of the cellular ROS level or the inhibition of the NF-κB signalling pathway by PUFA (Hagopian et al., 2010; Kremmyda et al., 2011; Marion-Letellier et al., 2015), as both were shown to mediate *cPLA2* gene

induction (Lin et al., 2016, 2011).

Metals, including Cd, have been reported to modulate the expression of various *CYPs* involved in cellular defence (Madejczyk et al., 2015; Olsvik et al., 2016; Reynders et al., 2006). We previously showed that the expression of the orphan *CYP20A1* gene was increased by PUFAs and decreased by methylmercury both in zebrafish larvae and RTL-W1 cells, suggesting CYP20A1 could represent a molecular target of interactive effects between PUFAs and some heavy metals (Ferain et al., 2018; Lemaire et al., 2016). In the present study, we observed that Cd significantly downregulated *CYP20A1*, but in EPA-enriched cells only. This suggests that the orphan *CYP20A1* may be involved in EPA-derived cytoprotection against Cd. Besides, in the absence of Cd challenge, EPA and AA enrichments significantly upregulated *CYP20A1* and downregulated *COX2* gene expression. These observations suggest that the orphan *CYP20A1* gene might have role in the eicosanoid cascade, as previously highlighted (Ferain et al., 2018).

Cd has been shown to cause abnormalities in the cytoskeleton architecture (Nawaz et al., 2005; Vergilio and De Melo, 2013) and influence the expression of structural constituents of the cytoskeleton (Dorts et al., 2012; Koskinen et al., 2004). However, the proteomic data of the present experiment revealed no such impact of Cd. In contrast, ALA, EPA and AA enrichments influenced the amount of different proteins of the cytoskeleton (cytokeratin-18, the intermediate filament protein ON3 and myosin-9). Still, the observed differences between PUFA-enriched cells and control cells disappeared after Cd exposure. The initial differences in the basal levels of some components of the cytoskeleton might have contributed to the PUFA-derived cytoprotection.

Stress response has a non-negligible energetic cost, which can be further increased by Cd since this metal has been shown to impair ATP production in rainbow trout (Adiele et al., 2012). A higher energy provision at the start of Cd exposure is thus likely to increase the ability of cells to cope with metal stress, as suggested by our observation on AA-enriched cells. Indeed, in absence of Cd, AA-enriched cells had a higher level of pyruvate kinase than control cells. Since this enzyme catalyses the tenth step of glycolysis (production of pyruvate and ATP from phosphoenolpyruvate and ADP) (Nelson et al., 2008), its upregulation may have provided AA-enriched cells with a high basal energy level, which may have contributed to the higher tolerance of AA-enriched cells towards Cd exposure.

5. Conclusion

The present study highlighted molecular interactions between PUFAs and Cd in fish liver cells. On the one hand, the fatty acid supply and, to a lesser extent, Cd influenced cellular fatty acid homeostasis and metabolism. On the other hand, the cellular fatty acid composition of fish liver cells modulated their tolerance to an acute Cd challenge. Enrichments in ALA, EPA, and, to a lesser extent, AA conferred cytoprotection while enrichment in LA had no impact on cell viability. Although the mechanisms of cytoprotection still remain to be fully understood, the present study ruled out the possibility that cytoprotection could result from a decreased Cd accumulation. It rather suggests that the PUFA-derived cytoprotection against Cd may occur through a reduction of the oxidative stress induced by Cd and a differential induction of the eicosanoid cascade. However, it remains difficult to discriminate between the direct and indirect mechanisms by which PUFAs modulate Cd toxicity. Other mechanisms such as modulations of the subcellular partitioning of Cd and of the cellular energy provision, as well as a reduction of the apoptosis triggered by Cd might also be involved. Further studies are needed to address these possibilities.

Acknowledgements

The research leading to these results has received funding from Belspo for the IAP AQUASTRESS project (P7/31), from the European Union Seventh Framework Programme (FP7/2007-2013) under grant agreement PIEF-GA-2012-332049 for the FISHSTRESS project and from the Fonds de la Recherche Scientifique (FNRS) (Aline Ferain is a F.R.I.A. Grant Holder of the FNRS). The authors acknowledge Catherine Rasse, Charlotte Baugnée, Gilles Tinant, Emmy Pequeur, Jolien Depecker, Hervé Degand and Jennifer Villers for their contribution to this work.

Appendix A. Supplementary data

Supplementary material related to this article can be found, in the online version, at doi:https://doi.org/10.1016/j.aquatox.2018.09.005.

References

Adiele, R.C., Stevens, D., Kamunde, C., 2012. Differential inhibition of electron transport chain enzyme complexes by cadmium and calcium in isolated rainbow trout (Oncorhynchus mykiss) hepatic mitochondria. Toxicol. Sci. 127, 110–119.
Amamou, F., Nemmiche, S., Meziane, R.K., Didi, A., Yazit, S.M., Chabane-Sari, D., 2015. Protective effect of olive oil and colocynth oil against cadmium-induced oxidative stress in the liver of Wistar rats. Food Chem. Toxicol. 78, 177–184.
Antoniali, G., Marcuzzi, F., Casarano, E., Tell, G., 2015. Cadmium treatment suppresses DNA polymerase delta catalytic subunit gene expression by acting on the p53 and Sp1 regulatory axis. DNA Repair 35, 90–105.
Arts, M.T., Kohler, C.C., 2009. Health and condition in fish: the influence of lipids on membrane competency and immune response. Lipids Aquat. Ecosyst. 237–256.
Baron, D., Houlgatte, R., Fostier, A., Guiguen, Y., 2005. Large-scale temporal gene expression profiling during gonadal differentiation and early gametogenesis in rainbow trout. Biol. Reprod. 73, 959–966.
Best, C.A., Laposata, M., Poios, V.G., Szczepiorkowski, Z.M., 2006. Method to assess fatty acid ethyl ester binding to albumin. Alcohol Alcohol. 41, 240–246.
Bligh, E.G., Dyer, W.J., 1959. A rapid method of total lipid extraction and purification. Can. J. Biochem. Physiol. 37, 911–917.
Bradford, M.M., 1976. A rapid and sensitive method for the quantitation of microgram quantities of protein utilizing the principle of protein-dye binding. Anal. Biochem. 72, 248–254.
Cartularo, L., Laulicht, F., Sun, H., Kluz, T., Freedman, J.H., Costa, M., 2015. Gene expression and pathway analysis of human hepatocellular carcinoma cells treated with cadmium. Toxicol. Appl. Pharmacol. 288, 399–408.
Casalino, E., Calzaretti, G., Sblano, C., Landriscina, C., 2002. Molecular inhibitory mechanisms of antioxidant enzymes in rat liver and kidney by cadmium. Toxicology 179, 37–50.
Ceyhun, S.B., Aksakal, E., Ekinci, D., Erdoğan, O., Beydemir, Ş., 2011. Influence of cobalt and zinc exposure on mRNA expression profiles of metallothionein and cytocrome P450 in rainbow trout. Biol. Trace Elem. Res. 144, 781–789.
Chen, Q.L., Gong, Y., Luo, Z., Zheng, J.L., Zhu, Q.L., 2013. Differential effect of waterborne cadmium exposure on lipid metabolism in liver and muscle of yellow catfish Pelteobagrus fulvidraco. Aquat. Toxicol. 142-143, 380–386.
Chen, Y.Y., Zhu, J.Y., Chan, K.M., 2014. Effects of cadmium on cell proliferation, apoptosis, and proto-oncogene expression in zebrafish liver cells. Aquat. Toxicol. 157, 196–206.
Chettri, J.K., Raida, M.K., Holten-Andersen, L., Kania, P.W., Buchmann, K., 2011. PAMP induced expression of immune relevant genes in head kidney leukocytes of rainbow trout (Oncorhynchus mykiss). Dev. Comp. Immunol. 35, 476–482.
Choi, J.H., Chang, H.W., Rhee, S.J., 2002. Effect of green tea catechin on arachidonic acid cascade in chronic cadmium-poisoned rats. Asia Pac. J. Clin. Nutr. 11, 292–297.
Chowdhury, M.J., Grosell, M., McDonald, D.G., Wood, C.M., 2003. Plasma clearance of cadmium and zinc in non-acclimated and metal-acclimated trout. Aquat. Toxicol. 64, 259–275.
Dagnelie, P., 2006. Statistique théorique et appliquée, Tome 2. Inference statistique à une et à deux dimensions. De boeck.
Dayeh, V.R., Schirmer, K., Bols, N.C., 2002. Applying whole-water samples directly to fish cell cultures in order to evaluate the toxicity of industrial effluent. Water Res. 36, 3727–3738.
Deane, E.E., Woo, N.Y.S., 2011. Advances and perspectives on the regulation and expression of piscine heat shock proteins. Rev. Fish Biol. Fish. 21, 153–185.
Dorts, J., Bauwin, A., Kestemont, P., Jolly, S., Sanchez, W., Silvestre, F., 2012. Proteasome and antioxidant responses in Cottus gobio during a combined exposure to heat stress and cadmium. Comp. Biochem. Physiol. - C Toxicol. Pharmacol. 155, 318–324.
Eriyamremu, G.E., Ojimogho, S.E., Asagba, S.O., Osagie, V.E., 2008. Palm oil induced changes in ocular tissue lipid peroxidation, antioxidant enzymes and ATPases of rabbits in cadmium toxicity. Food Chem. Toxicol. 46, 3155–3158.
Fadhlaoui, M., Couture, P., 2016. Combined effects of temperature and metal exposure on the fatty acid composition of cell membranes, antioxidant enzyme activities and lipid peroxidation in yellow perch (Perca flavescens). Aquat. Toxicol. 180, 45–55.
Fadhlaoui, M., Pierron, F., Couture, P., 2018. Temperature and metal exposure affect membrane fatty acid composition and transcription of desaturases and elongases in fathead minnow muscle and brain. Ecotoxicol. Environ. Saf. 148, 632–643.
Ferain, A., Bonnineau, C., Neefs, I., Rees, J.F., Larondelle, Y., De Schamphelaere, K.A.C., Debier, C., 2016. The fatty acid profile of rainbow trout liver cells modulates their tolerance to methylmercury and cadmium. Aquat. Toxicol. 177, 171–181.

Ferain, A., Bonnineau, C., Neefs, I., Das, K., Larondelle, Y., Rees, J.-F., Debier, C., Lemaire, B., 2018. Transcriptional effects of phospholipid fatty acid profile on rainbow trout liver cells exposed to methylmercury. Aquat. Toxicol. 199, 174–187.
Filimonova, V., Gonçalves, F., Marques, J.C., De Troch, M., Gonçalves, A.M.M., 2016. Fatty acid profiling as bioindicator of chemical stress in marine organisms: a review. Ecol. Indic. 67, 657–672.
Fox, M.R.S., 1979. Nutritional influences on metal toxicity: cadmium as a model toxic element. Environ. Health Perspect. 29, 95–104.
Frohnert, B.I., Bernlohr, D.A., 2000. Regulation of fatty acid transporters in mammalian cells. Prog. Lipid Res. 39, 83–107.
Gagné, F., Douville, M., André, C., Debenest, T., Talbot, A., Sherry, J., Hewitt, L.M., Frank, R.A., McMaster, M.E., Parrott, J., Bickerton, G., 2012. Differential changes in gene expression in rainbow trout hepatocytes exposed to extracts of oil sands process-affected water and the Athabasca River. Comp. Biochem. Physiol. Part C Toxicol. Pharmacol. 155, 551–559.
Go, Y.M., Roede, J.R., Orr, M., Liang, Y., Jones, D.P., 2014. Integrated redox proteomics and metabolomics of mitochondria to identify mechanisms of Cd toxicity. Toxicol. Sci. 139, 59–73.
Hagopian, K., Weber, K.L., Hwee, D.T., van Eenennaam, A.L., López-Lluch, G., Villalba, J.M., Burón, I., Navas, P., German, J.B., Watkins, S.M., Chen, Y., Wei, A., McDonald, R.B., Ramsey, J.J., 2010. Complex i-associated hydrogen peroxide production is decreased and electron transport chain enzyme activities are altered in n-3 enriched fat-1 mice. PLoS One 5, 1–11.
Hecht, B.C., Valle, M.E., Thrower, F.P., Nichols, K.M., 2014. Divergence in expression of candidate genes for the smoltification process between juvenile resident rainbow and anadromous steelhead trout. Mar. Biotechnol. (New York, N.Y.) 16, 638–656.
Jamwal, A., Naderi, M., Niyogi, S., 2016. An in vitro examination of selenium-cadmium antagonism using primary cultures of rainbow trout (Oncorhynchus mykiss) hepatocytes. Metallomics 8, 218–227.
Kamalam, B.S., Médale, F., Larroquet, L., Corraze, G., Panserat, S., 2013. Metabolism and fatty acid profile in fat and lean rainbow trout lines fed with vegetable oil: effect of carbohydrates. PLoS One 8, e76570.
Konar, V., Aydogmus, C., Orun, I., Kandemir, S., 2010. The Effects of Cadmium on fatty acid composition in the muscle and skin of juvenile rainbow trout (Oncorhynchus mykiss, Walbaum 1792). J. Anim. Vet. Adv. 9, 1191–1196.
Koskinen, H., Pehkonen, P., Vehniäinen, E., Krasnov, A., Rexroad, C., Afanasyev, S., Mölsa, H., Oikari, A., 2004. Response of rainbow trout transcriptome to model chemical contaminants. Biochem. Biophys. Res. Commun. 320, 745–753.
Kremmyda, L.S., Tvrzicka, E., Stankova, B., Zak, A., 2011. Fatty acids as biocompounds: their role in human metabolism, health and disease: a review. Part 2: fatty acid physiological roles and applications in human health and disease. Biomed. Pap. Med. Fac. Univ. Palacky Olomouc Czech. 155, 195–218.
Kudo, N., Waku, K., 1996. Cadmium suppresses Δ9 desaturase activity in rat hepatocytes. Toxicology 114, 101–111.
Leaver, M.J., Bautista, J.M., Björnsson, B.T., Jönsson, E., Krey, G., Tocher, D.R., Torstensen, B.E., 2008. Towards fish lipid nutrigenomics: current state and prospects for fin-fish aquaculture. Rev. Fish. Sci. 16, 73–94.
Lemaire, B., Kubota, A., O'Meara, C.M., Lamb, D.C., Tanguay, R.L., Goldstone, J.V., Stegeman, J.J., 2016. Cytochrome P450 20A1 in zebrafish: cloning, regulation and potential involvement in hyperactivity disorders. Toxicol. Appl. Pharmacol. 296, 73–84.
Lin, W.N., Lin, C.C., Cheng, H.Y., Yang, C.M., 2011. Regulation of cyclooxygenase-2 and cytosolic phospholipase A < inf > 2 < /inf > gene expression by lipopolysaccharide through the RNA-binding protein HuR: involvement of NADPH oxidase, reactive oxygen species and mitogen-activated protein kinases. Br. J. Pharmacol. 163, 1691–1706.
Lin, C.C., Lin, W.N., Cho, R.L., Wang, C.Y., Hsiao, L.D., Yang, C.M., 2016. TNF-α-induced cPLA < inf > 2 < /inf > expression via NADPH oxidase/reactive oxygen species-dependent NF-κB cascade on human pulmonary alveolar epithelial cells. Front. Pharmacol. 7.
Linhartova, P., Sampels, S., 2015. Combined incubation of Cadmium, docosahexaenoic and eicosapentaenoic acid results in increased uptake of cadmium and elevated docosapentaenoic acid content in Hepatocytes in vitro. Lipids Health Dis. 14.
Linhartova, P., Gazo, I., Sampels, S., 2016. Combined incubation of cadmium, docosahexaenoic and eicosapentaenoic acid affecting the oxidative stress and antioxidant response in human hepatocytes in vitro. Physiol. Res. 65, 609–616.
Livak, K.J., Schmittgen, T.D., 2001. Analysis of relative gene expression data using real-time quantitative PCR and the $2^{-\Delta\Delta CT}$ method. Methods 25, 402–408.
Lu, X.-J., Chen, J., Huang, Z.-A., Zhuang, L., Peng, L.-Z., Shi, Y.-H., 2011. Influence of acute cadmium exposure on the liver proteome of a teleost fish, ayu (Plecoglossus altivelis). Mol. Biol. Rep. 39 (3), 2851–2859.
Madejczyk, M.S., Baer, C.E., Dennis, W.E., Minarchick, V.C., Leonard, S.S., Jackson, D.A., Stallings, J.D., Lewis, J.A., 2015. Temporal changes in rat liver gene expression after acute cadmium and chromium exposure. PLoS One 10, e0127327.
Marancik, D., Gao, G., Paneru, B., Ma, H., Hernandez, A.G., Salem, M., Yao, J., Palti, Y., Wiens, G.D., 2014. Whole-body transcriptome of selectively bred, resistant-, control-, and susceptible-line rainbow trout following experimental challenge with Flavobacterium psychrophilum. Front. Genet. 5, 453.
Marion-Letellier, R., Savoye, G., Ghosh, S., 2015. Polyunsaturated fatty acids and inflammation. IUBMB Life 67, 659–667.
Mashek, D.G., Coleman, R.A., 2006. Cellular fatty acid uptake: the contribution of metabolism. Curr. Opin. Lipidol. 17, 274–278.
Matović, V., Buha, A., Dukić-Ćosić, D., Bulat, Z., 2015. Insight into the oxidative stress induced by lead and/or cadmium in blood, liver and kidneys. Food Chem. Toxicol. 78, 130–140.
McGeer, J.C., Niyogi, S., Scott Smith, D., 2011. Cadmium. Fish Physiol. Biochem. 125–184.
Mellery, J., Scalisi, F., Bonnineau, C., Kestemont, P., Rollin, X., Larondelle, Y., 2017. Impact of lignans on the polyunsaturated fatty acid metabolic processing in a rainbow trout (Oncorhynchus mykiss) cell line. Aquaculture 476, 106–110.
Mills, M.G., Gallagher, E.P., 2017. A targeted gene expression platform allows for rapid analysis of chemical-induced antioxidant mRNA expression in zebrafish larvae. PLoS One 12, e0171025.
Miyahara, T., Tonoyama, H., Watanabe, M., Okajima, A., Miyajima, S., Sakuma, T., Nemoto, N., Takayama, K., 2001. Stimulative effect of cadmium on prostaglandin E2 production in primary mouse osteoblastic cells. Calcif. Tissue Int. 68, 185–191.
Morcillo, P., Esteban, M.Á., Cuesta, A., 2016. Heavy metals produce toxicity, oxidative stress and apoptosis in the marine teleost fish SAF-1 cell line. Chemosphere 144, 225–233.
Moulis, J.M., 2010. Cellular mechanisms of cadmium toxicity related to the homeostasis of essential metals. Biometals 23, 877–896.
Nawaz, M., Manzl, C., Krumschnabel, G., 2005. In vitro toxicity of copper, cadmium, and chromium to isolated hepatocytes from carp, Cyprinus carpio L. Bull. Environ. Contam. Toxicol. 75, 652–661.
Nelson, D.L., Lehninger, A.L., Cox, M.M., 2008. Lehninger Principles of Biochemistry. W.H. Freeman.
Nøstbakken, O.J., Bredal, I.L., Olsvik, P.A., Huang, T.S., Torstensen, B.E., 2012. Effect of marine omega 3 fatty acids on methylmercury-induced toxicity in fish and mammalian cells in vitro. J. Biomed. Biotechnol. 2012.
Olsvik, P.A., Søfteland, L., Hevrøy, E.M., Rasinger, J.D., Waagbø, R., 2016. Fish pre-acclimation temperature only modestly affects cadmium toxicity in Atlantic salmon hepatocytes. J. Therm. Biol. 57, 21–34.
Olszowski, T., Baranowska-Bosiacka, I., Gutowska, I., Piotrowska, K., Mierzejewska, K., Korbecki, J., Kurzawski, M., Tarnowski, M., Chlubek, D., 2015. The effects of cadmium at low environmental concentrations on THP-1 macrophage apoptosis. Int. J. Mol. Sci. 16, 21410–21427.
Parente, L., Solito, E., 2004. Annexin 1: more than an anti-phospholipase protein. Inflamm. Res. 53, 125–132.
Peraza, M.A., Ayala-Fierro, F., Barber, D.S., Casarez, E., Rael, L.T., 1998. Effects of micronutrients on metal toxicity. Environ. Health Perspect. 106, 203–216.
Qiang, J., Tao, Y.F., He, J., Xu, P., Bao, J.W., Sun, Y.L., 2017. miR-122 promotes hepatic antioxidant defense of genetically improved farmed tilapia (GIFT, Oreochromis niloticus) exposed to cadmium by directly targeting a metallothionein gene. Aquat. Toxicol. 182, 39–48.
Reynders, H., van der Ven, K., Moens, L.N., van Remortel, P., De Coen, W.M., Blust, R., 2006. Patterns of gene expression in carp liver after exposure to a mixture of waterborne and dietary cadmium using a custom-made microarray. Aquat. Toxicol. 80, 180–193.
Schneider, A.C., Beguin, P., Bourez, S., Perfield, J.W., Mignolet, E., Debier, C., Schneider, Y.J., Larondelle, Y., 2012. Conversion of t11t13 CLA into C9t11 CLA in CACO-2 cells and inhibition by sterculic oil. PLoS One 7.
Sidak, Z., 1967. Rectangular confidence regions for the means of multivariate normal distributions. J. Am. Stat. Assoc. 62, 626–633.
Thévenod, F., Lee, W.K., 2013. Cadmium and cellular signaling cascades: interactions between cell death and survival pathways. Arch. Toxicol. 87, 1743–1786.
Tillman, T.S., Cascio, M., 2003. Effects of membrane lipids on ion channel structure and function. Cell Biochem. Biophys. 38, 161–190.
Tocher, D.R., 2003. Metabolism and functions of lipids and fatty acids in teleost fish. Rev. Fish. Sci. 11, 107–184.
Vandesompele, J., De Preter, K., Pattyn, F., Poppe, B., Van Roy, N., De Paepe, A., Speleman, F., 2002. Accurate normalization of real-time quantitative RT-PCR data by geometric averaging of multiple internal control genes. Genome Biol. 3 research0034.0031.
Vergilio, C.S., De Melo, E.J.T., 2013. Autophagy, apoptosis and organelle features during cell exposure to cadmiumč. Biocell 37, 45–54.
Villers, J., Savocco, J., Szopinska, A., Degand, H., Nootens, S., Morsomme, P., 2017. Study of the plasma membrane proteome dynamics reveals novel targets of the nitrogen regulation in yeast. Mol. Cell. Proteom. 16, 1652–1668.
Walker, P.A., Kille, P., Hurley, A., Bury, N.R., Hogstrand, C., 2008. An in vitro method to assess toxicity of waterborne metals to fish. Toxicol. Appl. Pharmacol. 230, 67–77.
Wallace, W.G., Lee, B.G., Luoma, S.N., 2003. Subcellular compartmentalization of Cd and Zn in two bivalves. I. Significance of metal-sensitive fractions (MSF) and biologically detoxified metal (BDM). Mar. Ecol. Prog. Ser. 249, 183–197.
Wang, W.X., Rainbow, P.S., 2006. Subcellular partitioning and the prediction of cadmium toxicity to aquatic organisms. Environ. Chem. 3, 395–399.
Wang, J., Zhu, H., Liu, X., Liu, Z., 2014. Oxidative stress and $Ca2+$ signals involved on cadmium-induced apoptosis in rat hepatocyte. Biol. Trace Elem. Res. 161, 180–189.
Wang, J., Zhang, H., Zhang, T., Zhang, R., Liu, R., Chen, Y., 2015. Molecular mechanism on cadmium-induced activity changes of catalase and superoxide dismutase. Int. J. Biol. Macromol. 77, 59–67.
Wood, Z.A., Schröder, E., Harris, J.R., Poole, L.B., 2003. Structure, mechanism and regulation of peroxiredoxins. Trends Biochem. Sci. 28, 32–40.
Zaykin, D.V., 2011. Optimally weighted Z-test is a powerful method for combining probabilities in meta-analysis. J. Evol. Biol. 24, 1836–1841.
Zhou, J., Stubhaug, I., Torstensen, B.E., 2010. Trans-membrane uptake and intracellular metabolism of fatty acids in Atlantic salmon (Salmo salar L.) hepatocytes. Lipids 45, 301–311.